

Stabilizer Rényi Entropy Encodes Fusion Rules of Topological Defects and Boundaries

Masahiro Hoshino^{1,*} and Yuto Ashida^{1,2}

¹*Department of Physics, The University of Tokyo, 7-3-1 Hongo, Bunkyo-ku, Tokyo 113-0033, Japan*

²*Institute for Physics of Intelligence, The University of Tokyo, 7-3-1 Hongo, Bunkyo-ku, Tokyo 113-0033, Japan*

(Dated: April 3, 2026)

We demonstrate that the stabilizer Rényi entropy (SRE), a computable measure of quantum magic, can serve as an information-theoretic probe for universal properties associated with conformal defects in one-dimensional quantum critical systems. Using boundary conformal field theory, we show that open boundaries manifest as a universal logarithmic correction to the SRE, whereas topological defects yield a universal size-independent term. When multiple defects are present, we find that the universal terms in the SRE faithfully reflect the defect-fusion rules that define a noninvertible symmetry algebra. These analytical predictions are corroborated by numerical calculations of the Ising model, where boundaries and topological defects are described by Cardy states and Verlinde lines, respectively.

Understanding universal properties of quantum resources is a cornerstone of modern physics. A paradigmatic example is entanglement, whose universal behavior has provided profound insights into various fields ranging from condensed matter to high-energy physics [1, 2]. In one-dimensional (1D) quantum critical systems described by conformal field theory (CFT) [3], for instance, the entanglement entropy (EE) exhibits a universal logarithmic scaling governed by the central charge [4–7]. This seminal result has been extended to systems with conformal defects, revealing an even richer tapestry of universal features [8–16].

Beyond entanglement, a crucial resource for universal quantum computation is nonstabilizerness (also known as quantum magic) [17–19]. The Gottesman-Knill theorem [20, 21] establishes that quantum circuits composed solely of Clifford gates can be efficiently simulated on a classical computer; thus, non-Clifford operations constitute the essential ingredient for quantum computational advantage. The stabilizer Rényi entropy (SRE) has recently emerged as a computable measure of nonstabilizerness [22, 23], enabling a surge of investigations into its role in quantum phase transitions [24–28], many-body dynamics and thermalization [29–37], measurement-induced phenomena [38–40], numerical methods [41–52], and other related topics [53–59]. In 1D critical systems, it has been shown that the SRE acquires a universal size-independent term gov-

erned by the Affleck-Ludwig g -factor [60], which encapsulates universal data of the underlying CFT [61].

Concurrently, the physics of conformal defects has garnered renewed interest in the context of noninvertible symmetries, where the concept of global symmetry has been generalized beyond the traditional group-theoretic framework [62–64]. In quantum field theories, generalized symmetries are embodied by topological defects, i.e., operators supported on extended manifolds that can be freely deformed without affecting physical observables [65]. The algebraic structure of these symmetries is captured by fusion rules of topological defects [66–69]. There, the fusion of noninvertible defects can yield a superposition of multiple defect channels, unlike their invertible counterparts. This richer algebraic structure potentially imposes unforeseen constraints on quantum resources in many-body systems, motivating the search for an information-theoretic probe of their manifestations.

The aim of this Letter is to analyze and propose the SRE as a natural probe for universal properties associated with conformal defects. Our central finding stems from a defining property of the SRE, namely, its invariance under Clifford unitaries. Specifically, we demonstrate that Clifford operations implement movement and fusion of topological defects in lattice models (Fig. 1(a)). Consequently, the SRE remains invariant when conformal defects are moved/fused, in contrast to other information quantities like EE, which are sensitive to defect locations and the choice of subsystems. For instance, in the case of the Ising CFT, EE fails to distinguish between the identity defect and the \mathbb{Z}_2 defect [12, 13], whereas the SRE can discern their distinct universal contributions. The SRE thus serves not merely as a probe but as a discovery tool; namely, through systematically searching for lattice operators that yield universal scaling behaviors, one can identify lattice realizations of topological defects and their fusion rules without prior knowledge.

Using boundary CFT, we show that factorizing defects, or equivalently, open boundaries induce a universal logarithmic correction to the SRE, whereas the influence of topological defects is captured by a universal size-independent term (Fig. 1(b)). Crucially, when multiple defects are present, the universal terms are governed by the underlying fusion

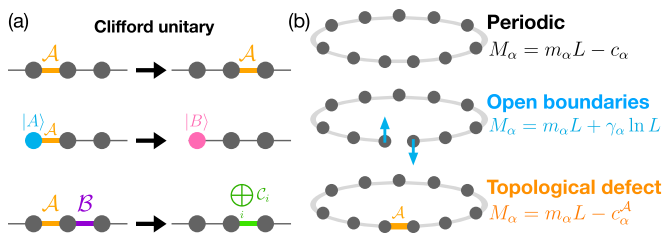


FIG. 1. (a) Conformal defects can be moved and fused by Clifford unitaries. The stabilizer Rényi entropy remains invariant under such operations, allowing it to directly probe the algebraic structure of defect fusion. (b) Open boundaries can be viewed as factorizing defects inserted in a periodic chain, whereas topological defects are created by locally altering the Hamiltonian.

rules. We corroborate these field-theoretical results with tensor-network calculations of the Ising model. Our work thus puts forward the SRE not only as a measure of a resource but as an information-theoretic probe for the algebraic structure of generalized symmetries.

From a broader perspective, our results provide insights into advancing tensor-network methods, such as the recently proposed Clifford augmented matrix product states [70–77]. For instance, we show that the Clifford unitaries used to disentangle critical spin chains [78, 79] can be understood as operations that move and fuse a topological defect with a boundary. Furthermore, given the growing experimental capability to manipulate defects and to measure magic-related quantities in quantum platforms [80, 81], our findings might motivate an experimental exploration for the physics of generalized symmetries.

Many-body quantum magic with conformal defects.— The constraints imposed by conformal invariance on line defects in a (1+1)D CFT have been studied both within continuum [82–91] and lattice [92–112]. A general conformal defect serves as an interface between two theories, CFT₁ and CFT₂, and is defined by the conservation of the energy-momentum tensor across it, i.e., $T_1 - \bar{T}_1 = T_2 - \bar{T}_2$, where T_i and \bar{T}_i are the holomorphic and antiholomorphic components of the energy-momentum tensor for CFT_{*i*}, respectively. Open boundaries are totally reflective, meaning the conservation law holds for each theory independently $T_i - \bar{T}_i = 0$. In contrast, topological defects are totally transmissive, satisfying $T_1 = T_2$ and $\bar{T}_1 = \bar{T}_2$. On a lattice, such conformal defects can be realized by locally modifying the Hamiltonian as illustrated in Fig. 1(b). In diagonal Virasoro minimal models, such as the Ising CFT, open boundaries are classified by Cardy states [113] and topological defects by Verlinde lines [114, 115].

We consider the ground state $|\psi\rangle$ of a critical spin chain of L qubits with conformal defects and measure its nonstabilizerness using the SRE defined as follows:

$$M_\alpha(\psi) = \frac{1}{1-\alpha} \ln \sum_{\vec{m}} \frac{\text{Tr}^{\alpha}[\sigma^{\vec{m}}\psi]}{2^L}. \quad (1)$$

Here, $\psi = |\psi\rangle\langle\psi|$ represents the density matrix corresponding to $|\psi\rangle$, and the L -qubit Pauli string $\sigma^{\vec{m}}$ is given by

$$\sigma^{\vec{m}} = \bigotimes_{j=1}^L \sigma^{m_{2j-1}m_{2j}} \quad (\vec{m} \in \{0, 1\}^{2L}), \quad (2)$$

where the Pauli matrices are labeled as $\sigma^{00} = I, \sigma^{10} = X, \sigma^{01} = Z$, and $\sigma^{11} = Y$. The SRE has the following key properties: (i) faithfulness, $M_\alpha(\psi) = 0$ if and only if $|\psi\rangle$ is a stabilizer state, (ii) stability under Clifford unitaries $C \in C_L$, $M_\alpha(C\psi C^\dagger) = M_\alpha(\psi)$, and (iii) additivity, $M_\alpha(\psi \otimes \phi) = M_\alpha(\psi) + M_\alpha(\phi)$. SREs with $\alpha \geq 2$ also satisfy monotonicity under stabilizer protocols [23]. We recall that the Clifford group C_L consists of unitary transformations that preserve the Pauli group, i.e., $C\sigma^{\vec{m}}C^\dagger = \sigma^{\vec{m}'}$ for $C \in C_L$; stabilizer states are constructed by applying Clifford unitaries to the product state $|0\rangle^{\otimes L}$.

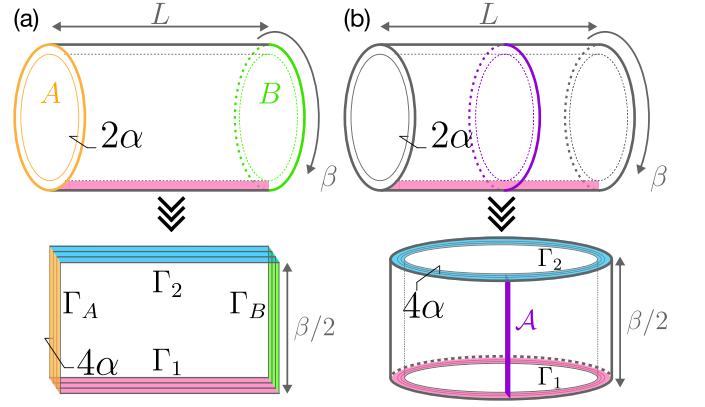


FIG. 2. (a) When the system has open boundaries, the partition function $Z_{2\alpha}$ of the 2α -component theory in Eq. (5) is defined on the cylinder with two ends A, B and a horizontal line defect due to the Bell projection at the fixed imaginary time $\tau = 0$. After folding, the cylinder becomes a rectangle with four boundaries, and the number of fields is double. (b) Torus of size $L \times \beta$ with a topological defect \mathcal{A} can be folded into a cylinder of circumference L and length $\beta/2$ with a vertical line defect. Periodicity in the spatial direction is implicit in the top panel.

Our CFT analysis starts by expressing the SRE as the participation entropy of a doubled state in the Bell basis [61]. Using the Choi-Jamiołkowski isomorphism [116, 117], we obtain

$$M_\alpha(\psi) = \frac{1}{1-\alpha} \ln \sum_{\vec{m}} \text{Tr}^\alpha[P^{\vec{m}}(\psi \otimes \psi^*)] - (\ln 2)L. \quad (3)$$

Here, $P^{\vec{m}} = \bigotimes_{j=1}^L |\text{Bell}^{m_{2j-1}m_{2j}}\rangle\langle\text{Bell}^{m_{2j-1}m_{2j}}|$ is the projection operator onto the Bell basis defined as $|\text{Bell}^{b_1b_2}\rangle = (|0b_1\rangle + (-1)^{b_2}|1\bar{b}_1\rangle)/\sqrt{2}$ with $b_1b_2 \in \{0, 1\}^2$. Thus, the SRE can be interpreted as the Rényi entropy of the classical probability distribution $p_{\vec{m}} = \text{Tr}[P^{\vec{m}}(\psi \otimes \psi^*)]$, up to a constant offset. In the path-integral formalism, a projection operator manifests as the Euclidean boundary action with an infinitely large coupling [118–128], which enforces the field configuration that can lead to a conformal defect along the *spatial* direction. Using the replica trick for $\alpha \in \mathbb{Z}_{\geq 2}$, we thus obtain

$$M_\alpha(\psi) = \frac{1}{1-\alpha} \ln \left(\frac{Z_{2\alpha}}{Z^{2\alpha}} \right) - (\ln 2)L, \quad (4)$$

$$\frac{Z_{2\alpha}}{Z^{2\alpha}} := \text{Tr} \left[\sum_{\vec{m}} (P^{\vec{m}})^{\otimes \alpha} (\psi \otimes \psi^*)^{\otimes \alpha} \right]. \quad (5)$$

Here, $Z_{2\alpha}$ is a partition function of the 2α -component CFT where the projection $\sum_{\vec{m}} (P^{\vec{m}})^{\otimes \alpha}$ yields a line defect at the imaginary-time slice (horizontal lines in top panels of Fig. 2), and Z is the original partition function for normalization.

In contrast, a defect contained in the Hamiltonian is described by a line defect along the *imaginary-time* direction. When this defect is factorizing, the geometry of the partition function $Z_{2\alpha}$ is a cylinder of length L and circumference β with two boundaries A and B at both ends (top panel of Fig. 2(a));

here, the inverse temperature β is understood to be taken infinitely large for the ground state. We use the folding trick to rewrite $Z_{2\alpha}$ as a partition function of 4α components on an $L \times \beta/2$ rectangle with the following four boundary conditions: Γ_1 at $\tau = 0$ subject to the projection $\sum_{\vec{m}} (P^{\vec{m}})^{\otimes \alpha}$, Γ_2 at $\tau = \beta/2$ corresponding to the artificial boundary created by the folding, and $\Gamma_{A,B}$ being the doubled boundary of the original one at each end A, B (bottom panel of Fig. 2(a)). Meanwhile, when the Hamiltonian contains a topological defect, the folding reduces $Z_{2\alpha}$ to a partition function of 4α components on a cylinder of circumference L and length $\beta/2$. The resulting cylinder has the boundaries Γ_1 and Γ_2 at the ends $\tau = 0, \beta/2$, while the topological defect denoted by \mathcal{A} is inserted along the imaginary-time direction (Fig. 2(b)).

One of our main results is that the SRE captures universal properties of conformal defects in qualitatively different ways, depending on the nature of defects. With factorizing defects, the SRE acquires the universal logarithmic correction due to the conical singularity at the corners [129–133]. Specifically, in the zero-temperature limit $\beta \rightarrow \infty$, we obtain

$$-\ln \frac{Z_{2\alpha}}{Z_{2\alpha}^0} = b_\alpha L + \gamma_\alpha \ln L + O(1), \quad (6)$$

where b_α is a nonuniversal line energy density associated with Γ_1 . The universal quantity γ_α is the sum of the contributions from each corner of the spacetime manifold. In general, for a corner of angle θ separating boundaries a and b , such contribution is given by [129]

$$\gamma^{ab} := \frac{c}{24} \left(\frac{\theta}{\pi} - \frac{\pi}{\theta} \right) + \frac{\pi}{\theta} h_{ab}, \quad (7)$$

where c is the central charge, and h_{ab} is the scaling dimension of the corresponding boundary condition changing operator (BCCO) [134, 135]. In the present geometry (Fig. 2(a)), the relevant corners are formed by the intersection of the spatial boundary $\Gamma_{A/B}$ and the measurement-induced boundary Γ_1 at $\tau = 0$ with the angle $\theta = \pi/2$, and we replace $c \rightarrow 4\alpha c$ because of the 4α components after folding. The contributions associated with the artificial boundary Γ_2 vanish by construction, while the two corners at the intersections of Γ_1 and $\Gamma_{A/B}$ contribute, yielding $\gamma_\alpha = \gamma^{1A} + \gamma^{1B}$.

In contrast, when topological defects are present, the logarithmic correction is absent and, instead, the universal data are encoded in a size-independent term:

$$-\ln \frac{Z_{2\alpha}}{Z_{2\alpha}^0} = b_\alpha L - \ln g_\alpha^A + o(1), \quad (8)$$

where $g_\alpha^A = \langle 0_A | \Gamma_1 \rangle$ is the g -factor given by the overlap between the boundary state $| \Gamma_1 \rangle$ and the ground state $| 0_A \rangle$ of the sector containing the topological defect \mathcal{A} (bottom panel of Fig. 2(b)). Here, the correction term $o(1)$ arises solely from finite-size effects (e.g., $O(L^{-1})$ corrections) and vanishes in the thermodynamic limit. This is in contrast to the nonuniversal $O(1)$ term in Eq. (6). Altogether, the SRE isolates the universal defect properties through distinct features:

a logarithmic correction with coefficient $(\alpha - 1)^{-1} \gamma_\alpha$ for factorizing defects, and a size-independent term $(1 - \alpha)^{-1} \ln g_\alpha^A$ for topological defects (cf. Eq. (4)).

Another key observation is that the SRE can probe dynamical properties such as fusion rules of conformal defects. This unique capability arises from the invariance of the SRE under Clifford unitaries. Indeed, the known transformations that move and fuse topological defects are implemented by Clifford unitaries [97, 105, 110]. Given that defect operations naturally map a Pauli string to another Pauli string, a defining feature of Clifford unitaries, we posit that the movement and fusion of a topological defect \mathcal{A} can be realized by Clifford unitaries.

This proposition leads to two primary consequences in the universal features of the SRE:

- (I) The universal coefficient of the logarithmic term is unchanged while a defect \mathcal{A} is moved and fused with either boundary; for instance, the coefficient for the pair of boundaries $(\mathcal{A} * |A\rangle, |B\rangle)$ is equivalent to that for $(|A\rangle, \mathcal{A} * |B\rangle)$ as illustrated in Fig. 3(a).
- (II) When the Hamiltonian contains multiple topological defects, the universal size-independent term is determined by the lowest-energy sector appearing in their fusion rule.

In property (I), we denote the fusion of a topological defect \mathcal{A} with a boundary A as $\mathcal{A} * |A\rangle$. Property (II) reflects the fact that a fusion rule $\mathcal{A} \otimes \mathcal{B} = \bigoplus_i C_i$ indicates that a Hamiltonian $H_{\mathcal{A} \otimes \mathcal{B}}$ with two topological defects can be mapped by Clifford unitaries to a direct sum of single-defect Hamiltonians $\bigoplus_i H_{C_i}$. Consequently, the lowest-energy sector gives the ground state of the original system, and the universal term in the SRE is governed by the g -factor of this defect channel. In what follows, we demonstrate these properties through a concrete analysis of the Ising CFT.

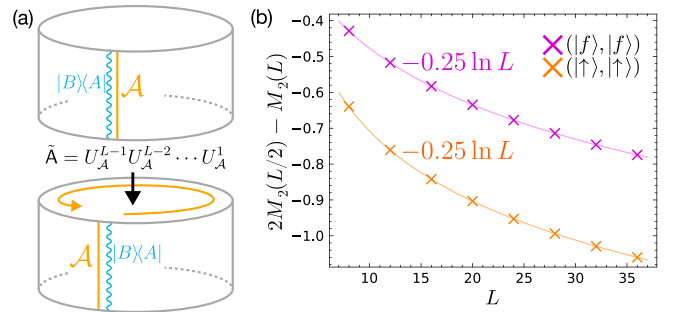


FIG. 3. (a) The SREs of open chains with the boundary pairs $(\mathcal{A} * |A\rangle, |B\rangle)$ and $(|A\rangle, \mathcal{A} * |B\rangle)$ are equivalent provided that one can move the defect \mathcal{A} from one side to the other and fuse it with the boundary via a Clifford unitary. (b) The universal logarithmic correction is extracted by fitting the data $2M_2(L/2) - M_2(L)$ as a function of the system size L , where $M_2(L)$ is the $\alpha = 2$ SRE of the L -qubit Ising critical state. The estimated coefficient agrees with the theoretical value $-1/4$ in both the $(|f\rangle, |f\rangle)$ and $(|\uparrow\rangle, |\uparrow\rangle)$ boundary pairs.

Factorizing defects in the Ising CFT.— A standard lattice model that realizes the $c = 1/2$ Ising CFT is the transverse field Ising model,

$$H = - \sum_{j=1}^L (Z_j Z_{j+1} + \lambda X_j), \quad (9)$$

where we impose periodic boundary conditions $X_j = X_{j+L}$ and $Z_j = Z_{j+L}$, λ represents the transverse field, and $\lambda = 1$ is the critical point. There are three conformal boundary states in the Ising CFT [113]: the free state $|f\rangle$, and the spin-up $|\uparrow\rangle$ and -down $|\downarrow\rangle$ states. Open boundaries, or equivalently, factorizing defects can be created by locally modifying the periodic chain. For example, a factorizing defect with free boundaries at both ends can be realized by setting $Z_L Z_1 \mapsto 0$, while a defect with spin-up boundaries at both ends corresponds to $Z_L Z_1 \mapsto -Z_L - Z_1$ in Eq. (9).

As inferred from Eq. (7), the field-theoretical derivation of the universal coefficient $\gamma_\alpha = \gamma^{1A} + \gamma^{1B}$ boils down to computing the scaling dimensions $h_{1A/B}$ of the BCCOs between Γ_1 and $\Gamma_{A/B}$ in the 4α -component replicated CFT. To this end, we map the doubled Ising CFT to a single S^1/\mathbb{Z}_2 CFT, which is the \mathbb{Z}_2 orbifold of the free-boson CFT compactified as $\phi \sim \phi + 2\pi$ [136, 137]. This mapping to the free-boson CFT makes the analysis of multicomponent theories more tractable. Under this mapping, the pair of free boundary states $|ff\rangle$ becomes the Dirichlet boundary state $|D(\pi/2)\rangle_{\text{orb}}$ localized at $\phi = \pi/2$ [92]. The corresponding boundary state in the replicated theory $Z_{2\alpha}$ is $|\Gamma_f\rangle = |D(\pi/2)\rangle_{\text{orb}}^{\otimes 2\alpha}$. Since Γ_1 corresponds to a mixed Dirichlet-Neumann boundary with a single component obeying the Neumann boundary condition [61], the scaling dimension of the BCCO between Γ_1 and Γ_f equals that of a twist (spin) field σ , which acts as changing a single boson field boundary from Dirichlet to Neumann. This allows us to determine $h_{1f} = 1/16$, which can also be confirmed by explicitly evaluating the amplitude $\langle \Gamma_f | e^{-\frac{\beta}{2} H_{\text{CFT}}} | \Gamma_1 \rangle$, where H_{CFT} is the CFT Hamiltonian on a ring (see Supplemental Material [138] for details).

Interestingly, property (I) above allows us to immediately determine other scaling dimensions such as $h_{1\uparrow}$ and $h_{1\downarrow}$. To see this, we recall that the Ising CFT has three topological defects: the identity 1 , the invertible \mathbb{Z}_2 defect η , and the noninvertible duality defect \mathcal{D} . The η and \mathcal{D} defects act on the boundary states as follows:

$$\eta * |f\rangle = |f\rangle, \quad \eta * |\uparrow\rangle = |\downarrow\rangle, \quad \eta * |\downarrow\rangle = |\uparrow\rangle, \quad (10)$$

$$\mathcal{D} * |f\rangle = |\uparrow\rangle + |\downarrow\rangle, \quad \mathcal{D} * |\uparrow\rangle = |f\rangle, \quad \mathcal{D} * |\downarrow\rangle = |f\rangle. \quad (11)$$

These relations are consistent with the following fusion rules among the topological defects:

$$\eta \otimes \eta = 1, \quad \eta \otimes \mathcal{D} = \mathcal{D} \otimes \eta = \mathcal{D}, \quad \mathcal{D} \otimes \mathcal{D} = 1 \oplus \eta. \quad (12)$$

The fusion rule (10) and property (I) of the SRE allows us to conclude that the SRE with the pair of boundaries $(|\uparrow\rangle, |f\rangle)$

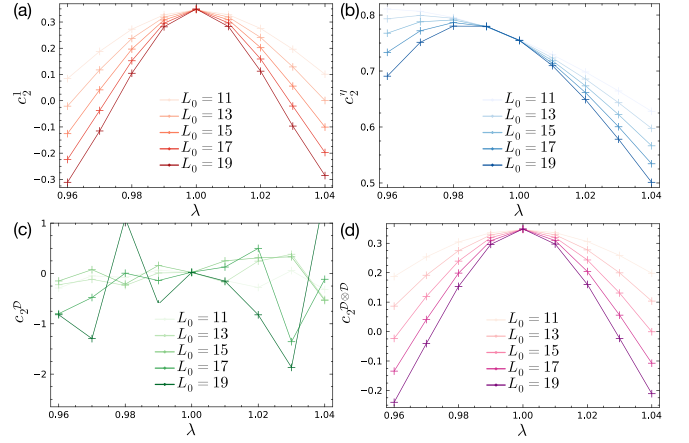


FIG. 4. Size-independent term c_2^A in the $\alpha = 2$ SRE of the closed chain with (a) the identity defect 1 , (b) the \mathbb{Z}_2 defect η , and (c) the duality defect \mathcal{D} . The numerical data were obtained using the replica-Pauli MPS method [45]. The data are extracted from the SRE fitted to $M_2 = m_2 L - c_2^A + r/L$ with $L \in \{L_0 - 5, L_0 - 3, \dots, L_0 + 5\}$ and $L_0 = 11, 13, \dots, 19$. The estimated universal values at the critical point $\lambda = 1$ are $c_2^1 = \ln \sqrt{2}$, $c_2^\eta = 0.755(1)$, and $c_2^{\mathcal{D}} = 0.020(3)$. (d) Size-independent term for two duality defects is extracted from the SRE of L qubits fitted to $M_2 = m_2(L - 1) - c_2^{\mathcal{D} \otimes \mathcal{D}}$, accounting for the defect \mathcal{T}^- . The universal value reads $c_2^{\mathcal{D} \otimes \mathcal{D}} = \ln \sqrt{2}$.

is equivalent to that with the pair $(|\downarrow\rangle, |f\rangle)$, implying $h_{1\uparrow} = h_{1\downarrow}$. Moreover, the relation (11) together with the property (I) indicates that the pair $(|f\rangle, |f\rangle)$ must give the same SRE as the pair $(|\uparrow\rangle, |\uparrow\rangle + |\downarrow\rangle)$. Since we have $h_{1\uparrow} = h_{1\downarrow}$, it follows that $h_{1\uparrow} = h_{1(\uparrow+\downarrow)}$. Consequently, we get $h_{1\uparrow} = h_{1\downarrow} = h_{1f} = 1/16$, indicating that, for all nine elementary factorizing defects, the SRE should behave as

$$M_\alpha(\psi) = m_\alpha L - \frac{1}{4} \ln L + O(1), \quad (13)$$

where we used Eq. (7) to obtain $\gamma^{1A/B} = (1 - \alpha)/8$ with $c = 2\alpha$, $\theta = \pi/2$, and $h_{1A/B} = 1/16$. This result is numerically verified by calculating the SRE of open chains using the replica-Pauli MPS method [45] (Fig. 3(b)).

It is noteworthy that local movement of the defects η and \mathcal{D} can be realized by $U_\eta^j = X_j$ and $U_{\mathcal{D}}^j = CZ_{j,j+1} H_j$, respectively, where H_j is the Hadamard gate and $CZ_{j,k}$ is the CZ gate, both being Clifford gates. Similarly, the fusion of defects can also be implemented by Clifford unitaries (see End Matter). Meanwhile, the global movement $\tilde{D} = U_{\mathcal{D}}^{L-1} U_{\mathcal{D}}^{L-2} \dots U_{\mathcal{D}}^1$ of the noninvertible duality defect \mathcal{D} satisfies $\tilde{D} X_j = Z_{j-1} Z_j \tilde{D}$ and $\tilde{D} Z_j Z_{j+1} = X_j \tilde{D}$ except at the ends of the chain. This observation gives a simple theoretical explanation of the disentangling Clifford unitary numerically found in Ref. [79]; it is nothing but the defect-movement operation \tilde{D} , which acts as the Kramers-Wannier transformation in the bulk while altering the boundaries.

Topological defects in the Ising CFT.— We next demonstrate that the SRE can also serve as a probe of topological defects and their fusion rules. In the Ising model, the insertion

of a topological defect η or \mathcal{D} corresponds to a local modification of the Hamiltonian, realized by $Z_j Z_{j+1} \mapsto -Z_j Z_{j+1}$ or $(Z_{j-1} Z_j + X_j) \mapsto Z_{j-1} X_j$, respectively. The presence of such a defect alters the sector of the CFT and its non-stabilizerness. This change can be detected by a universal size-independent term in the SRE:

$$c_\alpha^A = \frac{1}{\alpha - 1} \ln g_\alpha^A. \quad (14)$$

As shown in Figs. 4(a-c), the numerically estimated values of c_2^η and $c_2^{\mathcal{D}}$ are indeed distinct from the defect-free value [61]: $c_2^1 = \ln \sqrt{2}$, indicating that this universal quantity can distinguish different sectors. We remark that the failure of data collapse in Fig. 4(c) should be attributed to the fact that the perturbation by X_j in the off-critical region is no longer relevant in the sector containing the duality defect [67, 87, 139].

The use of the SRE becomes even more useful when applied to systems with multiple defects. One can successively move and fuse defects until a multidefect system effectively reduces to a single-defect problem. The fusion rules $\eta \otimes \eta = 1$ and $\eta \otimes \mathcal{D} = \mathcal{D}$, for instance, immediately imply the relations $c_\alpha^{\eta \otimes \eta} = c_\alpha^1$ and $c_\alpha^{\eta \otimes \mathcal{D}} = c_\alpha^{\mathcal{D}}$, respectively. A more subtle case arises from the noninvertible fusion rule of two duality defects, which on the lattice reads $\mathcal{D} \otimes \mathcal{D} = \mathcal{T}^-(1 \oplus \eta)$. This fusion leads to a direct sum of two defect channels 1 and η while the accompanying defect \mathcal{T}^- removes a site from the chain [105]. In the low-temperature limit $\beta \gg L$, the system selects the sector with the lowest energy, which corresponds to the identity channel 1 in the present case. Consequently, the SRE of the L -qubit ground state with two \mathcal{D} defects should match that of the defect-free ground state of size $L - 1$. This prediction is supported by our numerical results in Fig. 4(d), where we find that the universal term $c_2^{\mathcal{D} \otimes \mathcal{D}}$ matches the defect-free value c_2^1 . These results provide a numerical validation of property (II) postulated above. In fact, one can determine how many topological/factorizing defects are included in a given state by computing the SRE and using properties (I) and (II), and the additivity of the SRE.

Discussion.— Our results can be elevated to an active discovery tool for fusion rules of topological defects. The first step in determining fusion rules is the identification of the lattice realizations of topological defects. To this end, we first constrain the search space of candidate defect realizations based on physical requirements: Hermiticity, compatibility with movement with Clifford unitaries, and the transmissive nature of the topological defects. The resulting candidates are then classified into equivalence classes under Clifford unitaries to further reduce the search space. Next, we numerically compute the SRE for each candidate class. The emergence of a universal size-independent term—distinct from the logarithmic scaling characteristic of factorizing defects—serves as the signature of a topological defect. Finally, assuming that fusions are also implemented by Clifford unitaries, we apply Clifford unitaries to pairs of adjacent topological defects, and by checking whether it maps to a single defect or decouples a site to form a direct sum of defects, the fusion rules can be

determined. Consequently, our framework provides a systematic and practical tool for discovering topological defects and their algebraic structure in unknown critical spin chains. We refer the reader to the Supplemental Material [138] for a more detailed demonstration of this procedure.

Our findings open several avenues for future investigation. An immediate extension is to analyze the SRE in other CFTs possessing noninvertible symmetries, such as other minimal models or the compactified free boson. In the latter, investigating the SRE as a function of the compactification radius may offer a new perspective on T-duality. One could also explore models with higher central charge, for instance, by leveraging the mapping of the XX model to a doubled Ising CFT [110, 140, 141]. From a quantum information perspective, our work suggests that the SRE can quantify the magic resource cost of creating and manipulating topological defects, which might have implications for topological quantum computation. Extending our framework to two-dimensional systems, particularly those with topological order, could reveal how nonstabilizerness characterizes phases with noninvertible higher-form symmetries. While our specific results rely on the structure of $(1 + 1)$ D CFT, the appearance of universal data in subleading terms of the SRE is expected to be a more general feature, as observed in previous studies of participation entropy in higher dimensions [142–144]. Finally, studying the quench dynamics of the SRE in systems with defects may yield novel insights into the interplay between magic propagation and topological constraints.

Acknowledgments— We are grateful to Shunsuke Furukawa and Marcin Kalinowski for useful discussions. We especially thank Masaki Oshikawa for collaboration on related works [61, 124, 126]. We used the ITensor package [145, 146] for tensor-network calculations. M. H. was supported by FoPM, WINGS Program, the University of Tokyo. Y. A. acknowledges support from the Japan Society for the Promotion of Science through Grant No. JP19K23424 and from JST FOREST Program (Grant No. JPMJFR222U, Japan) and JST CREST (Grant No. JPMJCR23I2, Japan).

* hoshino-masahiro921@g.ecc.u-tokyo.ac.jp

- [1] L. Amico, R. Fazio, A. Osterloh, and V. Vedral, Entanglement in many-body systems, *Rev. Mod. Phys.* **80**, 517 (2008).
- [2] B. Zeng, X. Chen, D.-L. Zhou, and X.-G. Wen, *Quantum Information Meets Quantum Matter: From Quantum Entanglement to Topological Phases of Many-Body Systems* (Springer New York, 2019).
- [3] P. Di Francesco, P. Mathieu, and D. Sénéchal, *Conformal Field Theory* (Springer New York, 1997).
- [4] C. Holzhey, F. Larsen, and F. Wilczek, Geometric and renormalized entropy in conformal field theory, *Nuclear Physics B* **424**, 443 (1994).
- [5] G. Vidal, J. I. Latorre, E. Rico, and A. Kitaev, Entanglement in Quantum Critical Phenomena, *Phys. Rev. Lett.* **90**, 227902 (2003).
- [6] P. Calabrese and J. Cardy, Entanglement entropy and quantum

- field theory, *J. Stat. Mech.* **2004**, P06002 (2004).
- [7] P. Calabrese and J. Cardy, Entanglement entropy and conformal field theory, *J. Phys. A: Math. Theor.* **42**, 504005 (2009).
- [8] E. M. Brehm and I. Brunner, Entanglement entropy through conformal interfaces in the 2D Ising model, [arXiv:1505.02647 \[hep-th\]](#) (2015).
- [9] M. Gutperle and J. D. Miller, A note on entanglement entropy for topological interfaces in RCFTs, *J. High Energ. Phys.* **2016** (4), 176.
- [10] Y. Jiang, Entanglement entropy in integrable field theories with line defects. Part I. Topological defect, *J. High Energ. Phys.* **2017** (7), 127.
- [11] E. Cornfeld and E. Sela, Entanglement entropy and boundary renormalization group flow: Exact results in the Ising universality class, *Phys. Rev. B* **96**, 075153 (2017).
- [12] A. Roy and H. Saleur, Entanglement entropy in critical quantum spin chains with boundaries and defects, [arXiv:2111.07927 \[quant-ph\]](#) (2022).
- [13] A. Roy and H. Saleur, Entanglement Entropy in the Ising Model with Topological Defects, *Phys. Rev. Lett.* **128**, 090603 (2022).
- [14] D. Rogerson, F. Pollmann, and A. Roy, Entanglement entropy and negativity in the Ising model with defects, *J. High Energ. Phys.* **2022** (6), 165.
- [15] A. Roy and H. Saleur, Topological interfaces of Luttinger liquids, *Phys. Rev. B* **109**, L161107 (2024).
- [16] M. Gutperle, Y.-Y. Li, D. Rathore, and K. Roumpedakis, A note on entanglement entropy and topological defects in symmetric orbifold CFTs, *J. High Energ. Phys.* **2024** (9), 10.
- [17] S. Bravyi and A. Kitaev, Universal quantum computation with ideal Clifford gates and noisy ancillas, *Phys. Rev. A* **71**, 022316 (2005).
- [18] V. Veitch, S. A. Hamed Mousavian, D. Gottesman, and J. Emerson, The resource theory of stabilizer quantum computation, *New J. Phys.* **16**, 013009 (2014).
- [19] E. Chitambar and G. Gour, Quantum resource theories, *Rev. Mod. Phys.* **91**, 025001 (2019).
- [20] D. Gottesman, The Heisenberg Representation of Quantum Computers, [arXiv:quant-ph/9807006](#) (1998).
- [21] M. A. Nielsen and I. L. Chuang, *Quantum Computation and Quantum Information*, 10th ed. (Cambridge University Press, 2010).
- [22] L. Leone, S. F. E. Oliviero, and A. Hamma, Stabilizer Rényi Entropy, *Phys. Rev. Lett.* **128**, 050402 (2022).
- [23] L. Leone and L. Bittel, Stabilizer entropies are monotones for magic-state resource theory, *Phys. Rev. A* **110**, L040403 (2024).
- [24] S. F. E. Oliviero, L. Leone, and A. Hamma, Magic-state resource theory for the ground state of the transverse-field Ising model, *Phys. Rev. A* **106**, 042426 (2022).
- [25] P. S. Tarabunga, E. Tirrito, T. Chanda, and M. Dalmonte, Many-Body Magic Via Pauli-Markov Chains—From Criticality to Gauge Theories, *PRX Quantum* **4**, 040317 (2023).
- [26] M. Frau, P. S. Tarabunga, M. Collura, M. Dalmonte, and E. Tirrito, Nonstabilizerness versus entanglement in matrix product states, *Phys. Rev. B* **110**, 045101 (2024).
- [27] P. R. N. Falcão, P. S. Tarabunga, M. Frau, E. Tirrito, J. Zakrzewski, and M. Dalmonte, Nonstabilizerness in U(1) lattice gauge theory, *Phys. Rev. B* **111**, L081102 (2025).
- [28] M. Viscardi, M. Dalmonte, A. Hamma, and E. Tirrito, Interplay of entanglement structures and stabilizer entropy in spin models, [arXiv:2503.08620 \[quant-ph\]](#) (2025).
- [29] D. Rattacaso, L. Leone, S. F. E. Oliviero, and A. Hamma, Stabilizer entropy dynamics after a quantum quench, *Phys. Rev. A* **108**, 042407 (2023).
- [30] E. Tirrito, X. Turkeshi, and P. Sierant, Anticoncentration and magic spreading under ergodic quantum dynamics, [arXiv:2412.10229 \[quant-ph\]](#) (2024).
- [31] D. Szombathy, A. Valli, C. P. Moca, L. Farkas, and G. Zaránd, Independent stabilizer Rényi entropy and entanglement fluctuations in random unitary circuits, [arXiv:2501.11489 \[quant-ph\]](#) (2025).
- [32] J. Odavić, M. Viscardi, and A. Hamma, Stabilizer entropy in non-integrable quantum evolutions, [arXiv:2412.10228 \[quant-ph\]](#) (2025).
- [33] D. Szombathy, A. Valli, C. P. Moca, J. Asbóth, L. Farkas, T. Rakovszky, and G. Zaránd, Spectral Properties Versus Magic Generation in t-doped Random Clifford Circuits, [arXiv:2412.15912 \[quant-ph\]](#) (2025).
- [34] X. Turkeshi, A. Dymarsky, and P. Sierant, Pauli spectrum and nonstabilizerness of typical quantum many-body states, *Phys. Rev. B* **111**, 054301 (2025).
- [35] X. Turkeshi, E. Tirrito, and P. Sierant, Magic spreading in random quantum circuits, *Nat Commun* **16**, 2575 (2025).
- [36] D. Sticlet, B. Dóra, D. Szombathy, G. Zaránd, and C. P. Moca, Non-stabilizerness in open XXZ spin chains: Universal scaling and dynamics, [arXiv:2504.11139 \[quant-ph\]](#) (2025).
- [37] E. Tirrito, P. S. Tarabunga, D. S. Bhakuni, M. Dalmonte, P. Sierant, and X. Turkeshi, Universal Spreading of Nonstabilizerness and Quantum Transport, [arXiv:2506.12133 \[quant-ph\]](#) (2025).
- [38] P. S. Tarabunga and E. Tirrito, Magic transition in measurement-only circuits, [arXiv:2407.15939 \[cond-mat, physics:quant-ph\]](#) (2024).
- [39] P. Niroula, Phase transition in magic with random quantum circuits, *Nat. Phys.* (2024).
- [40] G. E. Fux, E. Tirrito, M. Dalmonte, and R. Fazio, Entanglement – nonstabilizerness separation in hybrid quantum circuits, *Phys. Rev. Res.* **6**, L042030 (2024).
- [41] T. Haug and L. Piroli, Quantifying nonstabilizerness of matrix product states, *Phys. Rev. B* **107**, 035148 (2023).
- [42] T. Haug and L. Piroli, Stabilizer entropies and nonstabilizerness monotones, *Quantum* **7**, 1092 (2023).
- [43] G. Lami and M. Collura, Nonstabilizerness via Perfect Pauli Sampling of Matrix Product States, *Phys. Rev. Lett.* **131**, 180401 (2023).
- [44] E. Tirrito, P. S. Tarabunga, G. Lami, T. Chanda, L. Leone, S. F. E. Oliviero, M. Dalmonte, M. Collura, and A. Hamma, Quantifying nonstabilizerness through entanglement spectrum flatness, *Phys. Rev. A* **109**, L040401 (2024).
- [45] P. S. Tarabunga, E. Tirrito, M. C. Bañuls, and M. Dalmonte, Nonstabilizerness via Matrix Product States in the Pauli Basis, *Phys. Rev. Lett.* **133**, 010601 (2024).
- [46] G. Passarelli, R. Fazio, and P. Lucignano, Nonstabilizerness of permutationally invariant systems, *Phys. Rev. A* **110**, 022436 (2024).
- [47] Z. Liu and B. K. Clark, Non-equilibrium Quantum Monte Carlo Algorithm for Stabilizer Rényi Entropy in Spin Systems, [arXiv:2405.19577 \[quant-ph\]](#) (2024).
- [48] M. Collura, J. D. Nardis, V. Alba, and G. Lami, The quantum magic of fermionic Gaussian states, [arXiv:2412.05367 \[quant-ph\]](#) (2024).
- [49] Y.-M. Ding, Z. Wang, and Z. Yan, Evaluating Many-Body Stabilizer Rényi Entropy by Sampling Reduced Pauli Strings: Singularities, Volume Law, and Nonlocal Magic, *PRX Quantum* **6**, 030328 (2025).
- [50] A. Russomanno, G. Passarelli, D. Rossini, and P. Lucignano, Efficient evaluation of the nonstabilizerness in unitary and monitored quantum many-body systems, [arXiv:2502.01431](#)

- [quant-ph] (2025).
- [51] S. B. Kožić and G. Torre, Computing Quantum Resources using Tensor Cross Interpolation, [arXiv:2502.06956 \[quant-ph\]](#) (2025).
- [52] P. S. Tarabunga and T. Haug, Efficient mutual magic and magic capacity with matrix product states, [arXiv:2504.07230 \[quant-ph\]](#) (2025).
- [53] J. Odavić, T. Haug, G. Torre, A. Hamma, F. Franchini, and S. M. Giampaolo, Complexity of frustration: A new source of non-local non-stabilizerness, *SciPost Phys.* **15**, 131 (2023).
- [54] X. Turkeshi, M. Schirò, and P. Sierant, Measuring nonstabilizerness via multifractal flatness, *Phys. Rev. A* **108**, 042408 (2023).
- [55] C. Cao, G. Cheng, A. Hamma, L. Leone, W. Munizzi, and S. F. E. Oliviero, Gravitational back-reaction is magical, [arXiv:2403.07056 \[hep-th\]](#) (2025).
- [56] S. Bera and M. Schirò, Non-Stabilizerness of Sachdev-Ye-Kitaev Model, [arXiv:2502.01582 \[quant-ph\]](#) (2025).
- [57] B. Jasser, J. Odavic, and A. Hamma, Stabilizer Entropy and entanglement complexity in the Sachdev-Ye-Kitaev model, [arXiv:2502.03093 \[quant-ph\]](#) (2025).
- [58] A. Sinibaldi, A. F. Mello, M. Collura, and G. Carleo, Non-stabilizerness of Neural Quantum States, [arXiv:2502.09725 \[quant-ph\]](#) (2025).
- [59] R. Smith, Z. Papić, and A. Hallam, Nonstabilizerness in kinetically constrained Rydberg atom arrays, *Phys. Rev. B* **111**, 245148 (2025).
- [60] I. Affleck and A. W. W. Ludwig, Universal noninteger “ground-state degeneracy” in critical quantum systems, *Phys. Rev. Lett.* **67**, 161 (1991).
- [61] M. Hoshino, M. Oshikawa, and Y. Ashida, Stabilizer Rényi Entropy and Conformal Field Theory, [arXiv:2503.13599 \[quant-ph\]](#) (2025).
- [62] J. Fröhlich, J. Fuchs, I. Runkel, and C. Schweigert, Kramers-Wannier Duality from Conformal Defects, *Phys. Rev. Lett.* **93**, 070601 (2004).
- [63] J. Fröhlich, J. Fuchs, I. Runkel, and C. Schweigert, Duality and defects in rational conformal field theory, *Nuclear Physics B* **763**, 354 (2007).
- [64] A. Davydov, L. Kong, and I. Runkel, Invertible defects and isomorphisms of rational CFTs, *Adv. Theor. Math. Phys.* **15**, 43 (2012).
- [65] D. Gaiotto, A. Kapustin, N. Seiberg, and B. Willett, Generalized global symmetries, *J. High Energy Phys.* **2015** (2), 1.
- [66] L. Bhardwaj and Y. Tachikawa, On finite symmetries and their gauging in two dimensions, *J. High Energy Phys.* **2018** (3), 189, [arXiv:1704.02330 \[hep-th\]](#).
- [67] C.-M. Chang, Y.-H. Lin, S.-H. Shao, Y. Wang, and X. Yin, Topological defect lines and renormalization group flows in two dimensions, *J. High Energy Phys.* **2019** (1), 26.
- [68] R. Thorngren and Y. Wang, Fusion category symmetry. Part I. Anomaly in-flow and gapped phases, *J. High Energy Phys.* **2024** (4), 132.
- [69] R. Thorngren and Y. Wang, Fusion category symmetry. Part II. Categoriosities at $c = 1$ and beyond, *J. High Energy Phys.* **2024** (7), 51.
- [70] G. Lami, T. Haug, and J. D. Nardis, Quantum State Designs with Clifford Enhanced Matrix Product States, [arXiv:2404.18751 \[quant-ph\]](#) (2024).
- [71] G. E. Fux, B. Béri, R. Fazio, and E. Tirrito, Disentangling unitary dynamics with classically simulable quantum circuits, [arXiv:2410.09001 \[quant-ph\]](#) (2024).
- [72] X. Qian, J. Huang, and M. Qin, Augmenting Density Matrix Renormalization Group with Clifford Circuits, *Phys. Rev. Lett.* **133**, 190402 (2024).
- [73] S. Masot-Llima and A. Garcia-Saez, Stabilizer Tensor Networks: Universal Quantum Simulator on a Basis of Stabilizer States, *Phys. Rev. Lett.* **133**, 230601 (2024).
- [74] X. Qian, J. Huang, and M. Qin, Clifford Circuits Augmented Time-Dependent Variational Principle, *Phys. Rev. Lett.* **134**, 150404 (2025).
- [75] A. F. Mello, A. Santini, and M. Collura, Clifford-dressed variational principles for precise Loschmidt echoes, *Phys. Rev. A* **111**, 052401 (2025).
- [76] A. C. Nakhil, B. Harper, M. West, N. Dowling, M. Seivior, T. Quella, and M. Usman, Stabilizer Tensor Networks with Magic State Injection, *Phys. Rev. Lett.* **134**, 190602 (2025).
- [77] L. Fu, H. Shang, J. Yang, and C. Guo, Clifford augmented density matrix renormalization group for *ab initio* quantum chemistry, *Phys. Rev. B* **112**, 195111 (2025).
- [78] M. Frau, P. S. Tarabunga, M. Collura, E. Tirrito, and M. Dalmonde, Stabilizer disentangling of conformal field theories, *SciPost Phys.* **18**, 165 (2025).
- [79] C. Fan, X. Qian, H.-C. Zhang, R.-Z. Huang, M. Qin, and T. Xiang, Disentangling critical quantum spin chains with Clifford circuits, *Phys. Rev. B* **111**, 085121 (2025).
- [80] D. Bluvstein, S. J. Evered, A. A. Geim, S. H. Li, H. Zhou, T. Manovitz, S. Ebadi, M. Cain, M. Kalinowski, D. Hangleiter, J. P. Bonilla Ataides, N. Maskara, I. Cong, X. Gao, P. Sales Rodriguez, T. Karolyshyn, G. Semeghini, M. J. Gullans, M. Greiner, V. Vuletić, and M. D. Lukin, Logical quantum processor based on reconfigurable atom arrays, *Nature* **626**, 58 (2024).
- [81] C. Monroe, W. C. Campbell, L.-M. Duan, Z.-X. Gong, A. V. Gorshkov, P. W. Hess, R. Islam, K. Kim, N. M. Linke, G. Pagano, P. Richerme, C. Senko, and N. Y. Yao, Programmable quantum simulations of spin systems with trapped ions, *Rev. Mod. Phys.* **93**, 025001 (2021).
- [82] K. Graham and G. M. T. Watts, Defect lines and boundary flows, *J. High Energy Phys.* **2004** (04), 019.
- [83] T. Quella, I. Runkel, and G. M. T. Watts, Reflection and transmission for conformal defects, *J. High Energy Phys.* **2007** (04), 095.
- [84] V. B. Petkova, Topological defects in CFT, *Phys. Atom. Nuclei* **76**, 1268 (2013).
- [85] M. Buican and A. Gromov, Anyonic Chains, Topological Defects, and Conformal Field Theory, *Commun. Math. Phys.* **356**, 1017 (2017).
- [86] C. Bachas, I. Brunner, and D. Roggenkamp, Fusion of critical defect lines in the 2D Ising model, *J. Stat. Mech.* **2013**, P08008 (2013).
- [87] Y.-H. Lin and S.-H. Shao, Duality Defect of the Monster CFT, [arXiv:1911.00042 \[hep-th\]](#) (2023).
- [88] C.-M. Chang, J. Chen, and F. Xu, Topological defect lines in two dimensional fermionic CFTs, *SciPost Phys.* **15**, 216 (2023).
- [89] Y. Choi, B. C. Rayhaun, Y. Sanghavi, and S.-H. Shao, Remarks on boundaries, anomalies, and noninvertible symmetries, *Phys. Rev. D* **108**, 125005 (2023).
- [90] Y. Choi, D.-C. Lu, and Z. Sun, Self-duality under gauging a non-invertible symmetry, *J. High Energy Phys.* **2024** (1), 142.
- [91] Y. Furuta, On the classification of duality defects in $c=2$ compact boson CFTs with a discrete group orbifold, [arXiv:2412.01319 \[hep-th\]](#) (2024).
- [92] M. Oshikawa and I. Affleck, Boundary conformal field theory approach to the critical two-dimensional Ising model with a defect line, *Nuclear Physics B* **495**, 533 (1997).
- [93] D. Aasen, R. S. K. Mong, and P. Fendley, Topological defects on the lattice: I. The Ising model, *J. Phys. A: Math. Theor.* **49**,

- 354001 (2016).
- [94] M. Hauru, G. Evenbly, W. W. Ho, D. Gaiotto, and G. Vidal, Topological conformal defects with tensor networks, *Phys. Rev. B* **94**, 115125 (2016), [arXiv:1512.03846 \[cond-mat\]](#).
- [95] J. Belletête, A. M. Gainutdinov, J. L. Jacobsen, H. Saleur, and T. S. Tavares, Topological defects in periodic RSOS models and anyonic chains, [arXiv:2003.11293 \[math-ph\]](#) (2020).
- [96] D. Aasen, P. Fendley, and R. S. K. Mong, Topological Defects on the Lattice: Dualities and Degeneracies, [arXiv:2008.08598 \[cond-mat\]](#) (2020).
- [97] Y. Fukusumi and S. Iino, Open spin chain realization of a topological defect in a one-dimensional Ising model: Boundary and bulk symmetry, *Phys. Rev. B* **104**, 125418 (2021).
- [98] S. Ashkenazi and E. Zohar, Duality as a feasible physical transformation for quantum simulation, *Phys. Rev. A* **105**, 022431 (2022).
- [99] L. Lootens, C. Delcamp, G. Ortiz, and F. Verstraete, Dualities in One-Dimensional Quantum Lattice Models: Symmetric Hamiltonians and Matrix Product Operator Intertwiners, *PRX Quantum* **4**, 020357 (2023).
- [100] J. Belletête, A. M. Gainutdinov, J. L. Jacobsen, H. Saleur, and T. S. Tavares, Topological defects in lattice models and affine Temperley-Lieb algebra, [arXiv:1811.02551 \[hep-th\]](#) (2023).
- [101] L. Li, M. Oshikawa, and Y. Zheng, Noninvertible duality transformation between symmetry-protected topological and spontaneous symmetry breaking phases, *Phys. Rev. B* **108**, 214429 (2023).
- [102] Y. Fukusumi, Protected edge modes based on the bulk and boundary renormalization group: A relationship between duality and generalized symmetry, [arXiv:2312.12887 \[hep-th\]](#) (2024).
- [103] S. Seifnashri, Lieb-Schultz-Mattis anomalies as obstructions to gauging (non-on-site) symmetries, *SciPost Phys.* **16**, 098 (2024).
- [104] M. Khan, S. A. B. Z. Khan, and A. Mohd, Quantum operations for Kramers-Wannier duality, [arXiv:2405.09361 \[hep-th\]](#) (2024).
- [105] N. Seiberg, S. Seifnashri, and S.-H. Shao, Non-invertible symmetries and LSM-type constraints on a tensor product Hilbert space, *SciPost Phys.* **16**, 154 (2024).
- [106] A. P. Mana, Y. Li, H. Sueno, and T.-C. Wei, Kennedy-Tasaki transformation and non-invertible symmetry in lattice models beyond one dimension, *Phys. Rev. B* **109**, 245129 (2024), [arXiv:2402.09520 \[cond-mat\]](#).
- [107] M. Sinha, F. Yan, L. Grans-Samuelsson, A. Roy, and H. Saleur, Lattice realizations of topological defects in the critical (1+1)-d three-state Potts model, *J. High Energy Phys.* **2024** (7), 225.
- [108] M. Okada and Y. Tachikawa, Noninvertible Symmetries Act Locally by Quantum Operations, *Phys. Rev. Lett.* **133**, 191602 (2024).
- [109] S. Seifnashri and S.-H. Shao, Cluster state as a non-invertible symmetry protected topological phase, [arXiv:2404.01369 \[cond-mat\]](#) (2025).
- [110] S. D. Pace, A. Chatterjee, and S.-H. Shao, Lattice T-duality from non-invertible symmetries in quantum spin chains, *SciPost Phys.* **18**, 121 (2025).
- [111] L. Li, M. Oshikawa, and Y. Zheng, Intrinsically/purely gapless-SPT from non-invertible duality transformations, *SciPost Phys.* **18**, 10.21468/scipostphys.18.5.153 (2025).
- [112] H.-C. Zhang and G. Sierra, Kramers-Wannier self-duality and non-invertible translation symmetry in quantum chains: A wave-function perspective, *J. High Energy Phys.* **2025** (5), [arXiv:2410.06727 \[cond-mat\]](#).
- [113] J. L. Cardy, Boundary conditions, fusion rules and the Verlinde formula, *Nuclear Physics B* **324**, 581 (1989).
- [114] E. Verlinde, Fusion rules and modular transformations in 2D conformal field theory, *Nuclear Physics B* **300**, 360 (1988).
- [115] V. B. Petkova and J. B. Zuber, Generalised twisted partition functions, *Physics Letters B* **504**, 157 (2001).
- [116] A. Jamiołkowski, Linear transformations which preserve trace and positive semidefiniteness of operators, *Reports on Mathematical Physics* **3**, 275 (1972).
- [117] M.-D. Choi, Completely positive linear maps on complex matrices, *Linear Algebra and its Applications* **10**, 285 (1975).
- [118] S. J. Garratt, Z. Weinstein, and E. Altman, Measurements Conspire Nonlocally to Restructure Critical Quantum States, *Phys. Rev. X* **13**, 021026 (2023).
- [119] X. Sun, H. Yao, and S.-K. Jian, New critical states induced by measurement, [arXiv:2301.11337 \[cond-mat, physics:quant-ph\]](#) (2023).
- [120] Z. Weinstein, R. Sajith, E. Altman, and S. J. Garratt, Non-locality and entanglement in measured critical quantum Ising chains, *Phys. Rev. B* **107**, 245132 (2023).
- [121] J. Y. Lee, C.-M. Jian, and C. Xu, Quantum Criticality Under Decoherence or Weak Measurement, *PRX Quantum* **4**, 030317 (2023).
- [122] Z. Yang, D. Mao, and C.-M. Jian, Entanglement in a one-dimensional critical state after measurements, *Phys. Rev. B* **108**, 165120 (2023).
- [123] S. Murciano, P. Sala, Y. Liu, R. S. K. Mong, and J. Alicea, Measurement-Altered Ising Quantum Criticality, *Phys. Rev. X* **13**, 041042 (2023).
- [124] Y. Ashida, Shunsuke Furukawa, and M. Oshikawa, System-environment entanglement phase transitions, *Phys. Rev. B* **110**, 094404 (2024).
- [125] Z. Zhang, Y. Zou, T. H. Hsieh, and S. Vijay, Universal Properties of Critical Mixed States from Measurement and Feedback, [arXiv:2503.09597 \[cond-mat\]](#) (2025).
- [126] M. Hoshino, M. Oshikawa, and Y. Ashida, Entanglement swapping in critical quantum spin chains, *Phys. Rev. B* **111**, 155143 (2025).
- [127] F. K. Popov and Y. Wang, Factorizing Defects from Generalized Pinning Fields, [arXiv:2504.06203 \[hep-th\]](#) (2025).
- [128] S. Naus, Y. Liu, S. Murciano, P. Sala, M. Endres, and J. Alicea, Practical roadmap to measurement-altered criticality in Rydberg arrays, [arXiv:2506.21963 \[quant-ph\]](#) (2025).
- [129] J. L. Cardy and I. Peschel, Finite-size dependence of the free energy in two-dimensional critical systems, *Nuclear Physics B* **300**, 377 (1988).
- [130] P. Kleban and I. Vassileva, Free energy of rectangular domains at criticality, *J. Phys. A: Math. Gen.* **24**, 3407 (1991).
- [131] Y. Imamura, H. Isono, and Y. Matsuo, Boundary States in the Open String Channel and CFT near a Corner, *Progress of Theoretical Physics* **115**, 979 (2006).
- [132] M. P. Zaletel, J. H. Bardarson, and J. E. Moore, Logarithmic Terms in Entanglement Entropies of 2D Quantum Critical Points and Shannon Entropies of Spin Chains, *Phys. Rev. Lett.* **107**, 020402 (2011).
- [133] J.-M. Stéphan, Shannon and Rényi mutual information in quantum critical spin chains, *Phys. Rev. B* **90**, 045424 (2014).
- [134] I. Affleck, Boundary condition changing operations in conformal field theory and condensed matter physics, *Nuclear Physics B - Proceedings Supplements* **58**, 35 (1997).
- [135] A. Recknagel and V. Schomerus, *Boundary Conformal Field Theory and the Worldsheet Approach to D-Branes*, 1st ed. (Cambridge University Press, 2013).
- [136] P. Di Francesco, H. Saleur, and J. Zuber, Critical Ising correlation functions in the plane and on the torus, *Nuclear Physics*

B **290**, 527 (1987).

- [137] P. Ginsparg, Curiosities at $c = 1$, *Nuclear Physics B* **295**, 153 (1988).
- [138] See supplemental material [url] for details of the boundary conformal field theory calculations and explanation on how to identify lattice realizations of topological defects, which includes ref. [147].
- [139] S.-H. Shao, What's Done Cannot Be Undone: TASI Lectures on Non-Invertible Symmetries, [arXiv:2308.00747](https://arxiv.org/abs/2308.00747) [hep-th] (2024).
- [140] R. Verresen, R. Thorngren, N. G. Jones, and F. Pollmann, Gapless Topological Phases and Symmetry-Enriched Quantum Criticality, *Phys. Rev. X* **11**, 041059 (2021).
- [141] L. Su, z_2 gauging and self-dualities of the XX model and its cousins, *Phys. Rev. B* **112**, 035105 (2025).
- [142] D. J. Luitz, F. Alet, and N. Laflorencie, Universal Behavior beyond Multifractality in Quantum Many-Body Systems, *Physical Review Letters* **112**, 057203 (2014).

- [143] D. J. Luitz, F. Alet, and N. Laflorencie, Shannon-Rényi entropies and participation spectra across three-dimensional (3) criticality, *Physical Review B* **89**, 165106 (2014).
- [144] G. Misguich, V. Pasquier, and M. Oshikawa, Finite-size scaling of the Shannon-Rényi entropy in two-dimensional systems with spontaneously broken continuous symmetry, *Physical Review B* **95**, 195161 (2017).
- [145] M. Fishman, S. White, and E. M. Stoudenmire, The ITensor Software Library for Tensor Network Calculations, *SciPost Phys. Codebases*, 004 (2022).
- [146] M. Fishman, S. White, and E. M. Stoudenmire, Codebase release 0.3 for ITensor, *SciPost Phys. Codebases*, 004 (2022).
- [147] N. Ishibashi, The boundary and crosscap states in conformal field theories, *Mod. Phys. Lett. A* **04**, 251 (1989).

End Matter

Fusion of the topological defects in the lattice model.— Here, we demonstrate that the movement and fusion of the topological defects in the lattice model can be implemented by Clifford unitaries. The defect Hamiltonian with the invertible \mathbb{Z}_2 defect η inserted at the bond $(L, 1)$ is written as

$$H_\eta^{(L,1)} = -(-Z_L Z_1 + X_1) - \sum_{j=2}^L (Z_{j-1} Z_j + X_j). \quad (\text{A1})$$

The topological nature of this defect allows us to move the defect by a local unitary $U_\eta^j = X_j$, such that

$$\begin{aligned} H_\eta^{(1,2)} &= U_\eta^1 H_\eta^{(L,1)} (U_\eta^1)^{-1} \\ &= -(-Z_1 Z_2 + X_2) - \sum_{j \neq 2} (Z_{j-1} Z_j + X_j). \end{aligned} \quad (\text{A2})$$

The local unitary U_η^j is called the movement operator, and its action is diagrammatically represented as

$$U_\eta^j = X_j = \begin{array}{c} \eta \\ \text{---} \bullet \text{---} \bullet \text{---} \bullet \text{---} \\ \text{---} \bullet \text{---} \bullet \text{---} \bullet \text{---} \\ \eta \end{array} \quad (\text{A3})$$

We note that, since the movement operator is a Clifford unitary, the η defect can be moved without consuming energy or magic.

We now consider the fusion of two η defects. After applying the movement operator, the two defects can be brought to adjacent bonds, resulting in the defect Hamiltonian

$$H_{\eta;\eta}^{(L,1):(1,2)} = - \sum_{i=1,2} (-Z_{j-1} Z_j + X_j) - \sum_{j=3}^L (Z_{j-1} Z_j + X_j). \quad (\text{A4})$$

The fusion of these defects can be implemented by a unitary $\lambda_{\eta \otimes \eta}^j = X_j$, which acts as

$$\lambda_{\eta \otimes \eta}^1 H_{\eta;\eta}^{(L,1):(1,2)} (\lambda_{\eta \otimes \eta}^1)^{-1} = H, \quad (\text{A5})$$

where we recall that H represents the Hamiltonian of the periodic chain in Eq. (9) in the main text. This is the lattice realization of the fusion rule $\eta \otimes \eta = 1$, which can be diagrammatically represented as

$$\lambda_{\eta \otimes \eta}^j = X_j = \begin{array}{c} \text{---} \bullet \text{---} \bullet \text{---} \bullet \text{---} \\ \text{---} \bullet \text{---} \bullet \text{---} \bullet \text{---} \\ \eta \quad \eta \end{array} \quad (\text{A6})$$

The defect Hamiltonian with the noninvertible duality defect \mathcal{D} inserted at the bond $(L, 1)$ is written as

$$H_{\mathcal{D}}^{(L,1)} = - \sum_{j=2}^L (Z_{j-1} Z_j + X_j) - Z_L X_1. \quad (\text{A7})$$

The movement operator for this defect is $U_{\mathcal{D}}^j = \text{CZ}_{j,j+1} H_j$, where H_j is the Hadamard gate and $\text{CZ}_{j,k}$ is the CZ gate. These unitaries act on the Pauli matrices as

$$H_j : X_j \mapsto Z_j, Z_j \mapsto X_j, \quad (\text{A8})$$

$$\text{CZ}_{j,k} : \begin{cases} X_j \mapsto X_j Z_k, & Z_j \mapsto Z_j \\ X_k \mapsto X_k Z_j, & Z_k \mapsto Z_k \end{cases} \quad (\text{A9})$$

Then, the diagrammatic representation for the movement operator $U_{\mathcal{D}}^j$ is given by

$$U_{\mathcal{D}}^j = \text{CZ}_{j,j+1} H_j = \begin{array}{c} \mathcal{D} \\ \text{---} \bullet \text{---} \bullet \text{---} \bullet \text{---} \\ \text{---} \bullet \text{---} \bullet \text{---} \bullet \text{---} \\ \mathcal{D} \end{array} \quad (\text{A10})$$

To identify the fusion of the η and \mathcal{D} defect, we consider the defect Hamiltonian

$$H_{\eta;\mathcal{D}}^{(L,1):(1,2)} = -(-Z_L Z_1 + X_1) - Z_1 X_2 - \sum_{j=3}^L (Z_{j-1} Z_j + X_j). \quad (\text{A11})$$

transforms as

$$\lambda_{\mathcal{D}^*|\uparrow} H_{|\uparrow;\mathcal{D}}^{(1,2)} (\lambda_{\mathcal{D}^*|\uparrow})^{-1} = H_{|f} \quad (\text{A28})$$

under the fusion operator

$$\lambda_{\mathcal{D}^*|\uparrow} = (U_{\mathcal{D}}^1)^{-1} = H_1 C Z_{1,2} = \dots \begin{array}{c} |f\rangle \\ \vdots \\ \text{---} \bullet \text{---} \\ \text{---} \bullet \text{---} \\ \vdots \\ |\uparrow\rangle \quad \mathcal{D} \\ \text{---} \bullet \text{---} \\ \text{---} \bullet \text{---} \\ \vdots \\ \text{---} \bullet \text{---} \\ \vdots \end{array}, \quad (\text{A29})$$

which implements $\mathcal{D}^*|\uparrow\rangle = |f\rangle$. Similarly, the fusion operator for the spin-down boundary $|\downarrow\rangle$ is given by $\lambda_{\mathcal{D}^*|\downarrow} = \lambda_{\mathcal{D}^*|\uparrow} X_1$. Finally, the fusion between the duality defect \mathcal{D} and the free boundary $|f\rangle$ can be described by the Hamiltonian

$$H_{|f;\mathcal{D}}^{(1,2)} = - \sum_{j=3}^{\infty} (Z_{j-1} Z_j + X_j) - Z_1 X_2 - X_1. \quad (\text{A30})$$

Using the fusion operator $\lambda_{\mathcal{D}^*|f} = (U_{\mathcal{D}}^1)^{-1}$, we obtain

$$\begin{aligned} & \lambda_{\mathcal{D}^*|f} H_{|f;\mathcal{D}}^{(1,2)} (\lambda_{\mathcal{D}^*|f})^{-1} \\ &= -Z_1 Z_2 - \sum_{j=2}^{\infty} (Z_j Z_{j+1} + X_j) \\ &= H_{\mathcal{T}^*|\uparrow} \otimes |0\rangle\langle 0|_1 + H_{\mathcal{T}^*|\downarrow} \otimes |1\rangle\langle 1|_1, \end{aligned} \quad (\text{A31})$$

where

$$H_{\mathcal{T}^*|\uparrow} = -Z_2 - \sum_{j=2}^{\infty} (Z_j Z_{j+1} + X_j), \quad (\text{A32})$$

$$H_{\mathcal{T}^*|\downarrow} = +Z_2 - \sum_{j=2}^{\infty} (Z_j Z_{j+1} + X_j), \quad (\text{A33})$$

are the Hamiltonians with spin-up and -down boundaries with one fewer lattice site. This explains how the superposition $|\uparrow\rangle + |\downarrow\rangle$ of the boundary is realized in the lattice model. The diagrammatic representation for this fusion is given by

$$\lambda_{\mathcal{D}^*|f} = (U_{\mathcal{D}}^1)^{-1} = H_1 C Z_{1,2} = \dots \begin{array}{c} |\uparrow\rangle + |\downarrow\rangle \\ \vdots \\ \text{---} \bullet \text{---} \\ \text{---} \bullet \text{---} \\ \vdots \\ |f\rangle \quad \mathcal{D} \\ \text{---} \bullet \text{---} \\ \text{---} \bullet \text{---} \\ \vdots \\ \text{---} \bullet \text{---} \\ \vdots \end{array}. \quad (\text{A34})$$

Altogether, we have demonstrated that all the fusions of the boundaries and topological defects in the Ising CFT can be implemented by Clifford unitaries.

Supplemental Material: Stabilizer Rényi Entropy Encodes Fusion Rules of Topological Defects and Boundaries

We provide the details of our BCFT analysis in obtaining the universal properties of the stabilizer Rényi entropy (SRE) in the presence of conformal defects. Specifically, we explicitly compute the scaling dimensions of the boundary condition changing operators (BCCOs) necessary to determine the universal terms contained in the SRE of the critical Ising model with open boundaries. We first construct conformal boundary states of $(N = 2\alpha)$ -component S^1/\mathbb{Z}_2 free-boson CFT which are consistent with the following boundary conditions $\Gamma_{1,2}$ [61] (see also Fig. 2(a) in the main text):

$$\Gamma_1 : \begin{cases} \sum_{i=1}^{2\alpha} \phi_i & \text{NBC} \\ \phi_1 - \phi_2 = 0 & \text{DBC} \\ \phi_2 - \phi_3 = 0 & \text{DBC} \\ \vdots \\ \phi_{2\alpha-1} - \phi_{2\alpha} = 0 & \text{DBC} \end{cases}, \quad (\text{S1})$$

and

$$\Gamma_2 : \begin{cases} \phi_i - \phi_{i+\alpha} = 0 & (i = 1, 2, \dots, \alpha) \text{ DBC} \\ \phi_i + \phi_{i+\alpha} & (i = 1, 2, \dots, \alpha) \text{ NBC} \end{cases}, \quad (\text{S2})$$

where NBC and DBC stand for Neumann and Dirichlet boundary conditions, respectively. Then, using the known correspondance between the boundary states in the double Ising CFT and the S^1/\mathbb{Z}_2 free-boson CFT [92], we compute the amplitudes between $\Gamma_{1,2}$ and $\Gamma_{A/B}$ to extract the scaling dimension of the BCCOs.

Construction of the boundary states in multicomponent S^1/\mathbb{Z}_2 free-boson CFT

To make the material self-contained, we here review the construction of a class of boundary states in the multicomponent S^1/\mathbb{Z}_2 free-boson CFT. Our construction builds upon the boundary states in the multicomponent S^1 free boson, from which we derive the corresponding boundary states in the multicomponent S^1/\mathbb{Z}_2 free boson through symmetrization.

The Lagrangian density of the bulk theory is

$$\mathcal{L} = \frac{1}{2\pi} (\partial_\mu \vec{\phi})^2 \quad (\mu = \tau, x), \quad (\text{S3})$$

where $\vec{\phi} = (\phi_1, \phi_2, \dots, \phi_N)$ is the N -component boson field. We describe the dual field of $\vec{\phi}$ as $\vec{\theta} = (\theta_1, \theta_2, \dots, \theta_N)$. These boson fields are compactified as

$$\vec{\phi} \sim \vec{\phi} + 2\pi \vec{R}, \quad \vec{\theta} \sim \vec{\theta} + 2\pi \vec{K}. \quad (\text{S4})$$

The vectors \vec{R} and \vec{K} belong to the following compactification lattice,

$$\Lambda = \left\{ \vec{x} \mid \vec{x} = \sum_{i=1}^N n_i \vec{e}_i, n_i \in \mathbb{Z} \right\}, \quad \Lambda^* = \left\{ \vec{y} \mid \vec{y} = \sum_{i=1}^N m_i \vec{f}_i, m_i \in \mathbb{Z} \right\}, \quad \vec{e}_i \cdot \vec{f}_j = \delta_{ij}, \quad (\text{S5})$$

respectively, where the lattice Λ^* is the dual of Λ , and $\vec{R} \cdot \vec{K} \in \mathbb{Z}$ is satisfied. For instance, when all the field components are decoupled, the compactification lattice is simply a square lattice. The fields $\vec{\phi}$ and $\vec{\theta}$ defined on the cylinder of circumference L can be expanded in the Fourier modes as follows:

$$\vec{\phi}(x, t) = \vec{\phi}_0 + \frac{2\pi}{L} \left(\vec{R}x + \frac{\vec{K}}{2}t \right) + \frac{1}{2} \sum_{n=1}^{\infty} \frac{1}{\sqrt{n}} \left(\vec{a}_n^L e^{-ik_n(x+t)} + \vec{a}_n^R e^{ik_n(x-t)} + \text{H.c.} \right), \quad (\text{S6})$$

$$\vec{\theta}(x, t) = \vec{\theta}_0 + \frac{2\pi}{L} \left(\vec{K}x + 2\vec{R}t \right) + \sum_{n=1}^{\infty} \frac{1}{\sqrt{n}} \left(\vec{a}_n^L e^{-ik_n(x+t)} - \vec{a}_n^R e^{ik_n(x-t)} + \text{H.c.} \right), \quad (\text{S7})$$

where $\vec{\phi}_0$ and $\vec{\theta}_0$ are the zero-mode operators, $\vec{a}_n^{L(R)}$ is a vector of the annihilation operators of left- (right-) moving oscillator modes having quantum number n , and $k_n = 2\pi n/L$. These operators satisfy the following commutation relations:

$$[(\vec{a}_n^s)_i, (\vec{a}_m^t)_j^\dagger] = \delta_{nm} \delta_{st} \delta_{ij} \quad (s, t \in \{L, R\}), \quad [(\vec{\phi}_0)_i, (\vec{K})_j] = i\delta_{ij}, \quad [(\vec{\theta}_0)_i, (\vec{R})_j] = i\delta_{ij}. \quad (\text{S8})$$

The Hamiltonian on the cylinder can be expressed in terms of these operators as follows:

$$H = \frac{2\pi}{L} \left(\vec{R}^2 + \frac{\vec{K}^2}{4} + \sum_{n=1}^{\infty} n [(\vec{a}_n^L)^\dagger \cdot \vec{a}_n^L + (\vec{a}_n^R)^\dagger \cdot \vec{a}_n^R] - \frac{N}{12} \right). \quad (\text{S9})$$

Its ground state is the simultaneous eigenstate of the winding modes \vec{R}, \vec{K} and the oscillators $\vec{a}_n^{L/R}$ with zero eigenvalues, and the ground-state energy is the Casimir energy $E_{\text{GS}}(L) = -\pi N/(6L)$.

The condition of conformal invariance of a boundary state $|\Gamma\rangle$ is given by

$$(L_m - \bar{L}_{-m}) |\Gamma\rangle = 0, \quad (\text{S10})$$

where L_m, \bar{L}_m are the Virasoro generators, expressed in terms of the Fourier modes as follows:

$$L_m = \frac{1}{2} \sum_l : \vec{\alpha}_{m-l}^L \cdot \vec{\alpha}_l^L :, \quad \bar{L}_m = \frac{1}{2} \sum_l : \vec{\alpha}_{m-l}^R \cdot \vec{\alpha}_l^R :. \quad (\text{S11})$$

Here, $: \dots :$ is the operator normal ordering, and the operators $\vec{\alpha}_n^{L,R}$ are defined as

$$\vec{\alpha}_n^L = \begin{cases} -i\sqrt{n}\vec{a}_n^L & (n > 0) \\ \frac{1}{2}\vec{K} + \vec{R} & (n = 0) \\ i\sqrt{n}(\vec{a}_{-n}^L)^\dagger & (n < 0) \end{cases}, \quad \vec{\alpha}_n^R = \begin{cases} -i\sqrt{n}\vec{a}_n^R & (n > 0) \\ \frac{1}{2}\vec{K} - \vec{R} & (n = 0) \\ i\sqrt{n}(\vec{a}_{-n}^R)^\dagger & (n < 0) \end{cases}. \quad (\text{S12})$$

A sufficient condition to satisfy Eq. (S10) is

$$(\vec{\alpha}_m^L - \mathcal{R}\vec{\alpha}_{-m}^R) |\Gamma\rangle = 0, \quad (\text{S13})$$

where \mathcal{R} is an $N \times N$ orthogonal matrix. This matrix \mathcal{R} becomes symmetric if each of the components satisfies either the DBC or the NBC. The states satisfying the sufficient condition (S13) for $m \neq 0$ can be given by the coherent states

$$S(\mathcal{R}) |\vec{R}, \vec{K}\rangle, \quad (\text{S14})$$

where

$$S(\mathcal{R}) = \exp \left[- \sum_{n=1}^{\infty} (\vec{a}_n^L)^\dagger \cdot \mathcal{R} (\vec{a}_n^R)^\dagger \right] \quad (\text{S15})$$

is the squeezing operator, and $|\vec{R}, \vec{K}\rangle$ are the oscillator vacua being the eigenstates of the winding modes \vec{R}, \vec{K} . These coherent states are known as the Ishibashi states in BCFT [135, 147]. The condition (S13) for $m = 0$ restricts the allowed states $|\vec{R}, \vec{K}\rangle$ to satisfy

$$\vec{K} + 2\vec{R} = \mathcal{R}(\vec{K} - 2\vec{R}). \quad (\text{S16})$$

Thus, any linear combination of the coherent states $S(\mathcal{R}) |\vec{R}, \vec{K}\rangle$ that satisfy (S16) are conformally invariant.

To correctly describe the theory with boundaries, physical boundary states must also satisfy the consistency condition known as the Cardy's consistency condition. To explain this, consider the transition amplitude between a pair of boundary states $|\mathcal{A}\rangle, |\mathcal{B}\rangle$ as follows:

$$Z_{AB}(q) = \langle \mathcal{B} | e^{-\frac{\beta}{2}H} | \mathcal{A} \rangle, \quad (\text{S17})$$

where $q = e^{2\pi i\tau}$ with $\tau = i\beta/L$ being the modular parameter. Under the modular transformation $\tau \rightarrow -1/\tau$ ($q \rightarrow \tilde{q} = e^{-2\pi i/\tau}$), which exchanges the direction of imaginary time and space, this amplitude is written as the trace over the Hilbert space \mathcal{H}_{AB} of the theory on a strip with boundary conditions \mathcal{A} and \mathcal{B} :

$$Z_{AB}(q) = \text{Tr} e^{-LH_{AB}}, \quad (\text{S18})$$

where H_{AB} is the corresponding CFT Hamiltonian. Given that the boundary conditions are conformally invariant, this Hilbert space decomposes into irreducible representations \mathcal{H}_h of the Virasoro algebra. Thus, the amplitude must be written as

$$Z_{AB}(q) = \sum_h n_{AB}^h \chi_h(\tilde{q}), \quad (\text{S19})$$

where

$$n_{AB}^h \in \mathbb{N}_0 \quad (\text{S20})$$

is a nonnegative integer interpreted as the number of primary fields with conformal weight h in the spectrum, and $\chi_h(\tilde{q})$ is the Virasoro character. When $\mathcal{A} = \mathcal{B}$ ($\mathcal{A} \neq \mathcal{B}$), we call the condition (S20) self (mutual) consistency condition. If the ground state of H_{AA} is unique, the boundary condition \mathcal{A} satisfies $n_{AA}^0 = 1$. We note that the consistency conditions cannot be satisfied by a single coherent state in Eq. (S14) alone. Thus, to construct physical boundary states, we must take appropriate linear combinations of the coherent states.

We now construct a class of the consistent boundary states for general mixed Dirichlet-Neumann boundary conditions. To begin with, we consider the simplest case of the fully DBC or fully NBC boundary states. The fully DBC corresponds to taking $\mathcal{R} = I$, and Eq. (S16) translates to $\vec{R} = \vec{0}$. The consistent boundary state is then

$$|D(\vec{\phi}_D)\rangle_c := g_D \sum_{\vec{K} \in \Lambda^*} e^{-i\vec{K} \cdot \vec{\phi}_D} S(I) |\vec{0}, \vec{K}\rangle, \quad (\text{S21})$$

where the coefficient $e^{-i\vec{K} \cdot \vec{\phi}_D}$ is introduced to ensure that this state is an eigenstate of $\vec{\phi}$ with eigenvalue $\vec{\phi}_D$. The subscript in $|\cdot\rangle_c$ stands for *circle* of the S^1 theory, which we use to distinguish it from the boundary states in the S^1/\mathbb{Z}_2 orbifold theory. The overall coefficient g_D plays the role of the g -factor, which can be given by the overlap of the boundary state with the ground state $|\text{GS}\rangle = |\vec{0}, \vec{0}\rangle$.

Similarly, the fully NBC corresponds to taking $\mathcal{R} = -I$, for which the boundary state is

$$|N(\vec{\theta}_D)\rangle_c := g_N \sum_{\vec{R} \in \Lambda} e^{-i\vec{R} \cdot \vec{\theta}_D} S(-I) |\vec{R}, \vec{0}\rangle, \quad (\text{S22})$$

where g_N is the corresponding g -factor. Since the NBC for $\vec{\phi}$ is equivalent to DBC for its dual $\vec{\theta}$, these states are labeled by the eigenvalue $\vec{\theta}_D$ of $\vec{\theta}$. The g -factors g_D and g_N are determined from the self-consistency condition and given by

$$g_D = 4^{-N/4} v_0(\Lambda)^{-1/2}, \quad g_N = v_0(\Lambda)^{1/2}, \quad (\text{S23})$$

where $v_0(\Lambda)$ is the unit-cell volume of the lattice Λ .

A general boundary state for mixed Dirichlet-Neumann boundary conditions can be expressed as

$$|\mathcal{R}(\vec{\phi}_D, \vec{\theta}_D)\rangle_c := g_{\mathcal{R}} \sum_{\vec{R} \in \Lambda_{\mathcal{R}}} \sum_{\vec{K} \in \Lambda_{\mathcal{R}}^*} e^{-i\vec{R} \cdot \vec{\theta}_D - i\vec{K} \cdot \vec{\phi}_D} S(\mathcal{R}) |\vec{R}, \vec{K}\rangle. \quad (\text{S24})$$

Here, $\Lambda_{\mathcal{R}}$ and $\Lambda_{\mathcal{R}}^*$ are subspaces of Λ and Λ^* that satisfy Eq. (S16). When each of the components satisfies either the DBC or the NBC, we can write $\mathcal{R} = \mathcal{P}_D - \mathcal{P}_N$, where $\mathcal{P}_{D/N}$ is the projection matrix onto the subspace $\mathcal{V}_{D/N}$ satisfying DBC/NBC. In terms of the projection matrices, Eq. (S16) becomes

$$\mathcal{P}_N \vec{K} = 0, \quad \mathcal{P}_D \vec{R} = 0, \quad (\text{S25})$$

and the subspaces $\Lambda_{\mathcal{R}}$ and $\Lambda_{\mathcal{R}}^*$ can be expressed as

$$\Lambda_{\mathcal{R}} = \Lambda \cap \mathcal{V}_N, \quad \Lambda_{\mathcal{R}}^* = \Lambda^* \cap \mathcal{V}_D. \quad (\text{S26})$$

We note that the g -factor $g_{\mathcal{R}}$ does not depend on the zero-mode phases $\vec{\phi}_D, \vec{\theta}_D$.

We now focus on the mixed boundary condition Γ_1 in Eq. (S1) and construct the corresponding boundary state $|\Gamma_1\rangle_c$ of the S^1 theory. In this case, the subspace \mathcal{V}_N is a one-dimensional space spanned by the vector $\vec{d} = (1, 1, \dots, 1)^T$, which corresponds to the NBC of the center of mass field $\sum_{i=1}^N \phi_i$. The complement of \mathcal{V}_N is the subspace \mathcal{V}_D , which corresponds to the DBC of the phase differences $\phi_i - \phi_{i+1}$. The zero-mode phases are simply given by $\vec{\phi}_D = 0$ and $\vec{\theta}_D = 0$. Since all the field components

are decoupled in the bulk theory, the compactification lattice Λ is a square lattice of lattice constant R , and the sublattices are written as

$$\Lambda_{\mathcal{R}} = \left\{ nR\vec{d} \mid n \in \mathbb{Z} \right\}, \quad \Lambda_{\mathcal{R}}^* = \left\{ \vec{K} \in \Lambda^* \mid \vec{d} \cdot \vec{K} = 0 \right\}. \quad (\text{S27})$$

To calculate the g -factor of $|\Gamma_1\rangle_c$, we consider the mutual consistency with the boundary state $|D(\vec{\phi}_D)\rangle_c$ in Eq. (S21). The amplitude between the two states reads

$$Z_{D\Gamma_1}(q) = {}_c\langle D(\vec{\phi}_D) | e^{-\frac{\beta}{2}H} | \Gamma_1 \rangle_c = \frac{\sqrt{2} g_D g_1^{\text{circ}}}{(\eta(q))^{N-1}} \sqrt{\frac{\eta(q)}{\theta_2(q)}} \sum_{\vec{K} \in \Lambda_{\mathcal{R}}^*} e^{i\vec{K} \cdot \vec{\phi}_D} q^{\vec{K}^2/8}, \quad (\text{S28})$$

where we express the g -factor of $|\Gamma_1\rangle_c$ by g_1^{circ} and use the Dedekind eta function $\eta(q)$ and the theta function $\theta_2(q)$. We define the eta function and the theta functions as follows:

$$\eta(q) = q^{1/24} \prod_{n=1}^{\infty} (1 - q^n), \quad (\text{S29})$$

$$\theta_2(q) = \sum_{n \in \mathbb{Z}} q^{(n+1/2)^2/2} = 2q^{1/8} \prod_{n=1}^{\infty} (1 - q^n)(1 + q^n)^2, \quad (\text{S30})$$

$$\theta_3(q) = \sum_{n \in \mathbb{Z}} q^{n^2/2} = \prod_{n=1}^{\infty} (1 - q^n)(1 + q^{n-1/2})^2, \quad (\text{S31})$$

$$\theta_4(q) = \sum_{n \in \mathbb{Z}} (-1)^n q^{n^2/2} = \prod_{n=1}^{\infty} (1 - q^n)(1 - q^{n-1/2})^2. \quad (\text{S32})$$

We note that the contribution $z_{DN} := \sqrt{\eta(q)/\theta_2(q)}$ originates from the amplitude of the center of mass field, and it is equivalent to the amplitude between the Dirichlet and Neumann boundary states of the single-component S^1 theory. By modular transformation $\tau \rightarrow -1/\tau$, the amplitude (S28) is rewritten in terms of \tilde{q} as

$$Z_{D\Gamma_1}(q) = \frac{\sqrt{2} g_D g_1^{\text{circ}} \times 4^{(N-1)/2}}{v_0(\Lambda_{\mathcal{R}}^*)(\eta(\tilde{q}))^{N-1}} \sqrt{\frac{\eta(\tilde{q})}{\theta_4(\tilde{q})}} \sum_{\vec{R} \in \tilde{\Lambda}_{\mathcal{R}}} \tilde{q}^{2\left(\vec{R} - \frac{\vec{\phi}_D}{2\pi}\right)^2}, \quad (\text{S33})$$

where $\tilde{\Lambda}_{\mathcal{R}}$ is the $(N-1)$ -dimensional lattice dual to $\Lambda_{\mathcal{R}}^*$. The mutual consistency leads to the following condition on the g -factors:

$$g_D g_1^{\text{circ}} \frac{\sqrt{2} \times 4^{(N-1)/2}}{v_0(\Lambda_{\mathcal{R}}^*)} = 1. \quad (\text{S34})$$

Thus, the amplitude (S33) can be written as the sum of Virasoro characters as follows:

$$Z_{D\Gamma_1}(q) = \frac{1}{(\eta(\tilde{q}))^N} \left(\sum_{n=1}^{\infty} \tilde{q}^{\frac{1}{4}(n-\frac{1}{2})^2} \right) \left(\sum_{\vec{R} \in \tilde{\Lambda}_{\mathcal{R}}} \tilde{q}^{2\left(\vec{R} - \frac{\vec{\phi}_D}{2\pi}\right)^2} \right). \quad (\text{S35})$$

Here, we used the identity

$$\sqrt{\frac{\eta(\tilde{q})}{\theta_4(\tilde{q})}} = \frac{\theta_2(\tilde{q}^{1/2})}{2\eta(\tilde{q})} = \frac{1}{\eta(\tilde{q})} \sum_{n=1}^{\infty} \tilde{q}^{\frac{1}{4}(n-\frac{1}{2})^2}. \quad (\text{S36})$$

We are now in a position to construct the boundary states in the multicomponent S^1/\mathbb{Z}_2 free-boson CFT. To this end, we symmetrize the boundary states of the S^1 theory constructed above so that the resulting states are invariant under the \mathbb{Z}_2 transformation: $\phi \rightarrow -\phi$. In the case of an N -component theory, the \mathbb{Z}_2 transformations form a group G with $|G| = 2^N$ elements, whose matrix representation in the N -dimensional vector space reads $a = \text{diag}(\pm 1, \pm 1, \dots, \pm 1)$ for $a \in G$. The

action of the transformation a on the boundary state is expressed as a unitary transformation $D(a)$ in the following manner

$$\begin{aligned}
D(a) |\mathcal{R}(\vec{\phi}_D, \vec{\theta}_D)\rangle_c &= g_{\mathcal{R}} \sum_{\vec{R} \in \Lambda_{\mathcal{R}}} \sum_{\vec{K} \in \Lambda_{\mathcal{R}}^*} e^{-i\vec{R} \cdot \vec{\theta}_D - i\vec{K} \cdot \vec{\phi}_D} S(a\mathcal{R}a) |a\vec{R}, a\vec{K}\rangle \\
&= g_{\mathcal{R}} \sum_{\vec{R} \in a\Lambda_{\mathcal{R}}} \sum_{\vec{K} \in a\Lambda_{\mathcal{R}}^*} e^{-i\vec{R} \cdot a\vec{\theta}_D - i\vec{K} \cdot a\vec{\phi}_D} S(a\mathcal{R}a) |\vec{R}, \vec{K}\rangle \\
&= |a\mathcal{R}a(a\vec{\phi}_D, a\vec{\theta}_D)\rangle_c,
\end{aligned} \tag{S37}$$

where we use $g_{\mathcal{R}} = g_{a\mathcal{R}a}$ and $a\Lambda_{\mathcal{R}} = \Lambda_{a\mathcal{R}a}$ to obtain the last line.

We start from the simplest case of the single-component ($N = 1$) S^1/\mathbb{Z}_2 free-boson CFT [92]. In this case, the orthogonal matrix $\mathcal{R} = \pm 1$ remains invariant under any $a \in G = \{\pm 1\}$, and the zero modes transform as $\phi_D \rightarrow -\phi_D, \theta_D \rightarrow -\theta_D$ under the action of $a = -1$. Thus, when the zero-mode parameters ϕ_D and θ_D take generic values, the symmetrized boundary states for $\mathcal{R} = \pm 1$ in the single-component S^1/\mathbb{Z}_2 theory are given by

$$|D(\phi_D)\rangle_{\text{orb}} = \frac{1}{\sqrt{2}}(|D(\phi_D)\rangle_c + |D(-\phi_D)\rangle_c), \quad |N(\theta_D)\rangle_{\text{orb}} = \frac{1}{\sqrt{2}}(|N(\theta_D)\rangle_c + |N(-\theta_D)\rangle_c). \tag{S38}$$

The coefficient $1/\sqrt{2}$ is determined from the self-consistency condition.

Meanwhile, when the zero-mode parameters take the fixed-point values of the transformation G , i.e., $\phi_D = \phi_E \in \{0, \pi R\}$ or $\theta_D = \theta_E \in \{0, \pi/R\}$, the boundary states $|D(\phi_E)\rangle_c, |D(-\phi_E)\rangle_c$ and $|N(\theta_E)\rangle_c, |N(-\theta_E)\rangle_c$ coincide and cannot satisfy the consistency condition. To address this issue, one can introduce the boundary states in the twisted sector, i.e., the S^1 free-boson CFT with anti-periodic boundary condition $\phi(x+L, t) = -\phi(x, t)$ on the cylinder. The boundary states in the twisted sector are labeled by the fixed-point values ϕ_E, θ_E , which are the only allowed eigenvalues due to the anti-periodicity. We denote the boundary states in the twisted sector by the subscript in $|\cdot\cdot\cdot\rangle_t$. Accordingly, the consistent boundary states within the S^1/\mathbb{Z}_2 theory can be constructed by the following combination of the fixed-point boundary states in the untwisted and twisted sectors:

$$|D(\phi_E)\rangle_{\text{orb}} = \frac{1}{\sqrt{2}} |D(\phi_E)\rangle_c \pm 2^{-1/4} |D(\phi_E)\rangle_t, \quad |N(\theta_E)\rangle_{\text{orb}} = \frac{1}{\sqrt{2}} |N(\theta_E)\rangle_c \pm 2^{-1/4} |N(\theta_E)\rangle_t. \tag{S39}$$

Here, the coefficient $1/\sqrt{2}$ for the untwisted sector is determined from the mutual consistency with the boundary states in Eq. (S38), and the coefficient $2^{-1/4}$ for the twisted sector is determined from the self-consistency.

We next consider a multicomponent theory with $N \geq 2$, for which the orthogonal matrix \mathcal{R} transforms nontrivially under the action of G , requiring a more careful analysis of boundary states. We can categorize these boundary states based on both the structure of \mathcal{R} and the values of $\vec{\phi}_D, \vec{\theta}_D$ into the following cases:

1. Block-diagonal $\mathcal{R} = \mathcal{R}_1 \oplus \mathcal{R}_2 \oplus \cdots \oplus \mathcal{R}_k$ (with appropriate exchange of the components).
2. Not block-diagonal and,
 - (a) for all $a \in G$, $a\vec{\phi}_D \neq \vec{\phi}_D$ and $a\vec{\theta}_D \neq \vec{\theta}_D$,
 - (b) $\vec{\phi}_D = -\vec{\phi}_D$ and $\vec{\theta}_D = -\vec{\theta}_D$ under the compactification.

Case 1 corresponds to the situation where the action of G is disconnected, and the boundary states are factorized into boundary states of the connected subspace of G . Case 2(a) corresponds to the boundary states with generic zero modes, which can be expressed as

$$|\mathcal{R}(\vec{\phi}_D, \vec{\theta}_D)\rangle_{\text{orb}} = \frac{1}{\sqrt{|G|}} \sum_{a \in G} D(a) |\mathcal{R}(\vec{\phi}_D, \vec{\theta}_D)\rangle_c. \tag{S40}$$

In contrast, case 2(b) corresponds to the zero-mode parameters at the fixed points $\vec{\phi}_D = \vec{\phi}_E \in \pi\Lambda \cap \mathcal{V}_D$ and $\vec{\theta}_D = \vec{\theta}_E \in \pi\Lambda^* \cap \mathcal{V}_N$, for which the boundary states transform identically under both a and $-a$, allowing us to make G -invariant states by symmetrizing over the subgroup $G_0 = G/\{\pm I\}$. In the similar manner as in the single-component case, one can construct the consistent boundary state in this case by including the boundary state in the twisted sector as follows:

$$|\mathcal{R}(\vec{\phi}_E, \vec{\theta}_E)\rangle_{\text{orb}} = \sum_{b \in G_0} D(b) \left[\frac{1}{\sqrt{|G|}} |\mathcal{R}(\vec{\phi}_E, \vec{\theta}_E)\rangle_c \pm 2^{-N/4} |\mathcal{R}(\vec{\phi}_E, \vec{\theta}_E)\rangle_t \right], \tag{S41}$$

where the coefficients are determined from the consistency conditions.

Building on these general constructions, we can now determine the boundary states $|\Gamma_{1,2}\rangle_{\text{orb}}$, which are necessary to analyze the SRE. First, we recall that $|\Gamma_1\rangle_{\text{orb}}$ corresponding to the mixed boundary condition in Eq. (S1) has the zero modes $\vec{\phi}_D = \vec{\phi}_E = \vec{0}$ and $\vec{\theta}_D = \vec{\theta}_E = \vec{0}$, which are at the fixed points. We can thus use Eq. (S41) to obtain

$$|\Gamma_1\rangle_{\text{orb}} = \frac{1}{\sqrt{|G|}} \sum_{b \in G_0} D(b) |\Gamma_1\rangle_c \pm 2^{-N/4} \sum_{b \in G_0} D(b) |\Gamma_1\rangle_t, \quad (\text{S42})$$

where $|\Gamma_1\rangle_t$ represents the corresponding boundary state in the twisted sector. The boundary state $|\Gamma_2\rangle_{\text{orb}}$ in Eq. (S2) corresponding to the artificially created boundary is factorized into two-component boundary states, each of which is equivalent to $|\Gamma_1\rangle_{\text{orb}}$ at $\alpha = 1$.

For later use, we also explicitly construct the twisted sector boundary states. The boson field $\vec{\phi}$ in the twisted sector can be expanded as follows:

$$\vec{\phi}(x, t) = \vec{\phi}_0 + \sum_{\substack{r \in \mathbb{Z} + \frac{1}{2} \\ r > 0}} \frac{1}{\sqrt{4r}} \left(\vec{b}_r^L e^{-ik_r(x+t)} + \vec{b}_r^R e^{ik_r(x-t)} + \text{H.c.} \right), \quad (\text{S43})$$

with oscillator modes satisfying $[(\vec{b}_r^s)_i, (\vec{b}_u^t)_j] = \delta_{st} \delta_{ru} \delta_{ij}$. Here $\vec{\phi}_0$ takes values in $\pi\Lambda_0$, where Λ_0 is the unit-cell of Λ :

$$\Lambda_0 = \left\{ \vec{x} \mid \vec{x} = \sum_{i=1}^N \varepsilon_i \vec{e}_i, \varepsilon_i = 0, 1 \right\}. \quad (\text{S44})$$

The Hamiltonian in the twisted sector is:

$$H_t = \frac{2\pi}{L} \left(\sum_{\substack{r \in \mathbb{Z} + \frac{1}{2} \\ r > 0}} r [(\vec{b}_r^L)^\dagger \cdot \vec{b}_r^L + (\vec{b}_r^R)^\dagger \cdot \vec{b}_r^R] + \frac{N}{24} \right). \quad (\text{S45})$$

The oscillator vacua are labeled either by the eigenvalues of $\vec{\phi}_0$ as $|\pi\vec{R}\rangle_t$ ($\vec{R} \in \Lambda_0$) or by its dual $\vec{\theta}_0$ as $|\pi\vec{K}\rangle_t$ ($\vec{K} \in \Lambda_0^*$), where Λ_0^* is defined similarly to Λ_0 . These vacua are related by:

$$|\pi\vec{R}\rangle_t = \frac{1}{\sqrt{2^N}} \sum_{\vec{K} \in \Lambda_0^*} e^{-i\pi\vec{K} \cdot \vec{R}} |\pi\vec{K}\rangle_t, \quad |\pi\vec{K}\rangle_t = \frac{1}{\sqrt{2^N}} \sum_{\vec{R} \in \Lambda_0} e^{i\pi\vec{K} \cdot \vec{R}} |\pi\vec{R}\rangle_t. \quad (\text{S46})$$

The boundary states in the untwisted sector are eigenstates of the zero-mode operators $\mathcal{P}_D \vec{\phi}_0, \mathcal{P}_N \vec{\theta}_0$, and we need to obtain the corresponding boundary states also in the twisted sector. Since the compactification lattice Λ is a square lattice, the state $|\pi\vec{R}\rangle_t$ is in the form of a tensor product of the boundary states for each component: $|\pi\vec{R}\rangle_t = |\pi R_1 \varepsilon_1\rangle |\pi R_2 \varepsilon_2\rangle_t \cdots |\pi R_N \varepsilon_N\rangle_t$. We can exchange the basis of this Hilbert space so that the state $|\pi\vec{R}\rangle_t$ is expressed as a tensor product $|\pi\mathcal{P}_D \vec{R}\rangle_t |\pi\mathcal{P}_N \vec{R}\rangle_t$. Then, we rotate the state in \mathcal{V}_N to create the eigenstate of the operator $\mathcal{P}_N \vec{\theta}_D$ as

$$|\pi\mathcal{P}_N \vec{K}\rangle_t = \frac{1}{\sqrt{2^{\dim \mathcal{V}_N}}} \sum_{\vec{R} \in \mathcal{P}_N \Lambda_0} e^{i\pi\vec{K} \cdot \vec{R}} |\pi\mathcal{P}_N \vec{R}\rangle_t. \quad (\text{S47})$$

The boundary state $|\pi\mathcal{P}_D \vec{R}\rangle_t |\pi\mathcal{P}_N \vec{K}\rangle_t$ is now an eigenstate of the two operators $\mathcal{P}_D \vec{\phi}_0, \mathcal{P}_N \vec{\theta}_0$ by construction. Then, the boundary state $|\mathcal{R}(\vec{\phi}_E, \vec{\theta}_E)\rangle_t$ in the twisted sector corresponding to the fixed point boundary state $|\mathcal{R}(\vec{\phi}_E, \vec{\theta}_E)\rangle$ ($\vec{\phi}_E \in \pi\Lambda_0 \cap \mathcal{V}_E, \vec{\theta}_E \in \pi\Lambda_0^* \cap \mathcal{V}_N$) in the untwisted sector is expressed as

$$|\mathcal{R}(\vec{\phi}_E, \vec{\theta}_E)\rangle_t = S_t(\mathcal{R}) |\vec{\phi}_E\rangle_t |\vec{\theta}_E\rangle_t, \quad (\text{S48})$$

where

$$S_t(\mathcal{R}) = \exp \left(- \sum_r (\vec{b}_r^L)^\dagger \cdot \mathcal{R}(\vec{b}_r^R)^\dagger \right) \quad (\text{S49})$$

is the squeezing operator in the twisted sector. The group G acts on the twisted sector in the same way as it acts on the untwisted sector boundary states: $D(a) |\mathcal{R}(\vec{\phi}_E, \vec{\theta}_E)\rangle_t = |a\mathcal{R}a(a\vec{\phi}_E, a\vec{\theta}_E)\rangle_t$.

Calculation of the scaling dimensions

The scaling dimension of a BCCO can be extracted from the transition amplitude between boundary states. It equals the lowest conformal weight appearing in the decomposition of the amplitude into Virasoro characters.

For the pairs of Cardy states in the Ising CFT, we can express their boundary states in terms of the S^1/\mathbb{Z}_2 free-boson CFT boundary states as follows:

$$|ff\rangle = |D(\pi/2)\rangle_{\text{orb}} = \frac{1}{\sqrt{2}}(|D(\pi/2)\rangle_c + |D(-\pi/2)\rangle_c), \quad (\text{S50})$$

$$|\uparrow\uparrow\rangle = |D(0+)\rangle_{\text{orb}} = \frac{1}{\sqrt{2}}|D(0)\rangle_c + 2^{-1/4}|D(0)\rangle_t, \quad (\text{S51})$$

$$|\downarrow\downarrow\rangle = |D(0-)\rangle_{\text{orb}} = \frac{1}{\sqrt{2}}|D(0)\rangle_c - 2^{-1/4}|D(0)\rangle_t. \quad (\text{S52})$$

Since the boundary states in the partition function $Z_{2\alpha}$ (Eq. (4)) are a 2α -fold product of these pairs, they can be written as

$$|\Gamma_f\rangle = |D(\pi/2)\rangle_{\text{orb}}^{\otimes N} = \frac{1}{\sqrt{|G|}} \sum_{a \in G} D(a) |D((\pi/2)\vec{a})\rangle_c, \quad (\text{S53})$$

$$|\Gamma_\uparrow\rangle = |D(0+)\rangle_{\text{orb}}^{\otimes N} = \frac{1}{\sqrt{|G|}} |D(\vec{0})\rangle_c + \dots + 2^{-N/4} |D(\vec{0})\rangle_t, \quad (\text{S54})$$

$$|\Gamma_\downarrow\rangle = |D(0-)\rangle_{\text{orb}}^{\otimes N} = \frac{1}{\sqrt{|G|}} |D(\vec{0})\rangle_c + \dots + 2^{-N/4} |D(\vec{0})\rangle_t. \quad (\text{S55})$$

Let us first calculate the scaling dimension h_{1f} , which can be extracted from the amplitude between $|\Gamma_1\rangle$ and $|\Gamma_f\rangle$:

$$\begin{aligned} Z_{1f}(q) &= \frac{1}{|G|} \sum_{a \in G} \sum_{b \in G_0} c \langle D((\pi/2)\vec{a}) | D(a) e^{-\frac{\beta}{2}H} D(b) | \Gamma_1 \rangle_c \\ &= \frac{1}{2} \sum_{a \in G} c \langle D((\pi/2)a\vec{a}) | e^{-\frac{\beta}{2}H} | \Gamma_1 \rangle_c \\ &= \frac{1}{2} \sum_{a \in G} \frac{g_D g_1^{\text{circ}}}{(\eta(q))^{N-1}} \sqrt{\frac{\eta(q)}{\theta_2(q)}} \sum_{\vec{K} \in \Lambda_{\mathcal{R}}^*} e^{i\vec{K} \cdot \mathcal{P}_D \vec{\phi}_D} q^{\vec{K}^2/8} \quad (\vec{\phi}_D = \frac{\pi}{2} a\vec{a}) \\ &= \frac{1}{2} \sum_{a \in G} \frac{1}{(\eta(\tilde{q}))^N} \left(\sum_{n=1}^{\infty} \tilde{q}^{\frac{1}{4}(n-\frac{1}{2})^2} \right) \sum_{\vec{R} \in \tilde{\Lambda}_{\mathcal{R}}} \tilde{q}^{2(\vec{R}-\frac{1}{4}\mathcal{P}_D a\vec{a})^2}. \end{aligned} \quad (\text{S56})$$

The lowest conformal weight $h = 1/16$ comes from the term with $a = \pm I$ in the sum, which leads to

$$h_{1f} = \frac{1}{16}. \quad (\text{S57})$$

Similarly, we can also explicitly calculate the amplitude between $|\Gamma_1\rangle$ and $|\Gamma_{\uparrow/\downarrow}\rangle$. Since $N = 2\alpha$ is even, the sign in front of the twisted sector boundary state does not matter, and both \uparrow and \downarrow yield the same amplitude. The calculation reads

$$\begin{aligned} Z_{1\uparrow/\downarrow}(q) &= \sum_{b \in G_0} \left[\frac{1}{|G|} c \langle D(\vec{0}) | e^{-\frac{\beta}{2}H} D(b) | \Gamma_1 \rangle_c + 2^{-N/2} {}_t \langle D(\vec{0}) | e^{-\frac{\beta}{2}H_t} D(b) | \Gamma_1 \rangle_t \right] \\ &= \frac{1}{2} \frac{1}{(\eta(\tilde{q}))^N} \left(\sum_{n=1}^{\infty} \tilde{q}^{\frac{1}{4}(n-\frac{1}{2})^2} \right) \sum_{\vec{R} \in \tilde{\Lambda}_{\mathcal{R}}} \tilde{q}^{2\vec{R}^2} + \frac{1}{2} \frac{\tilde{q}^{1/16}}{(\eta(\tilde{q}))^N} \left(\sum_{n \in \mathbb{Z}} (-1)^n \tilde{q}^{n^2+n/2} \right) \left(\sum_{n \in \mathbb{Z}} (-1)^n \tilde{q}^{n^2} \right)^{N-1}. \end{aligned} \quad (\text{S58})$$

Here, the contribution from the twisted sector is computed as

$$\begin{aligned}
{}_t\langle D(\vec{0})|e^{-\frac{\beta}{2}H_t}|\Gamma_1\rangle_t &= q^{N/48} \left(\frac{1}{\sqrt{2}} \prod_{n=1}^{\infty} \frac{1}{1+q^{n-1/2}} \right) \left(\prod_{n=1}^{\infty} \frac{1}{1-q^{n-1/2}} \right)^{N-1} \\
&= \frac{\theta_2(e^{i\pi/2}, q^{1/2})}{2\eta(q)} \left(\frac{\theta_2(q^{1/2})}{2\eta(q)} \right)^{N-1} \\
&= \frac{\tilde{q}^{1/16}}{\sqrt{2}\eta(\tilde{q})} \theta_4(\tilde{q}^{1/2}, \tilde{q}^2) \left(\frac{\theta_4(\tilde{q}^2)}{\sqrt{2}\eta(\tilde{q})} \right)^{N-1} \\
&= 2^{-N/2} \frac{\tilde{q}^{1/16}}{(\eta(\tilde{q}))^N} \left(\sum_{n \in \mathbb{Z}} (-1)^n \tilde{q}^{n^2+n/2} \right) \left(\sum_{n \in \mathbb{Z}} (-1)^n \tilde{q}^{n^2} \right)^{N-1}, \tag{S59}
\end{aligned}$$

where the theta functions $\theta_2(y, q)$ and $\theta_4(y, q)$ are defined as follows:

$$\theta_2(y, q) = \sum_{n \in \mathbb{Z}} y^{n+1/2} q^{\frac{1}{2}(n-\frac{1}{2})^2}, \tag{S60}$$

$$\theta_4(y, q) = \sum_{n \in \mathbb{Z}} (-1)^n y^n q^{n^2/2}. \tag{S61}$$

These two functions are related by the modular transformation as

$$\theta_2(y, q) = \frac{1}{\sqrt{-i\tau}} \theta_4(y^{-1/\tau}, \tilde{q}) e^{-\pi iz^2/\tau} \quad (y = e^{2\pi iz}). \tag{S62}$$

The lowest conformal weight contained in the amplitude (S58) is $h = 1/16$, and therefore the scaling dimensions are

$$h_{1\uparrow} = h_{1\downarrow} = \frac{1}{16}. \tag{S63}$$

We can also calculate the scaling dimensions of the BCCO between $|\Gamma_2\rangle$ and $|\Gamma_{f,\uparrow,\downarrow}\rangle$ and confirm that the coefficient of the logarithmic contribution in the partition function is indeed zero, as expected from the fact that $|\Gamma_2\rangle$ is the artificial boundary created by the folding. To see this, the key point is that the scaling dimensions $h_{1f} = h_{1\uparrow} = h_{1\downarrow}$ do not depend on the number of components $N = 2\alpha$. Since $|\Gamma_2\rangle$ is the α -fold product of $|\Gamma_1\rangle$ at $\alpha = 1$, we can deduce that the scaling dimensions also multiply by α . Thus, we have

$$h_{2f} = h_{2\uparrow} = h_{2\downarrow} = \frac{\alpha}{16}, \tag{S64}$$

and the coefficient reads

$$\gamma^{2f} = \gamma^{2\uparrow} = \gamma^{2\downarrow} = \frac{2\alpha}{24} \left(\frac{1}{2} - 2 \right) + 2 \times \frac{\alpha}{16} = 0. \tag{S65}$$

We note that if one can identify the boundary state in the two-component S^1/\mathbb{Z}_2 free-boson CFT that describes the boundary obtained by folding the product of topological defects $1 \otimes 1, \eta \otimes \eta, \mathcal{D} \otimes \mathcal{D}$ in the two-component Ising CFT, it should be possible to confirm that the conical singularity is absent even when we fold at the topological defect to make the geometry a rectangle. To the best of our knowledge, in contrast to the single-component Ising CFT [92], such correspondence is not established, and we leave this problem for future work.

USING SRE FOR A SYSTEMATIC IDENTIFICATION OF LATTICE REALIZATIONS AND FUSION RULES

In this section, we establish a systematic procedure to identify lattice realizations of topological defects and determine their fusion rules without prior knowledge, utilizing the SRE as a diagnostic probe. This approach allows for the discovery of non-invertible symmetries and their algebraic structures directly from the lattice Hamiltonian.

We search for topological defects in the critical Ising chain by considering a local modification of the Hamiltonian, specifically on the bond connecting sites L and 1 . We assume the defect Hamiltonian H_{L1} acts non-trivially only on these two sites and takes a general form of the sum of Pauli strings:

$$H_{L1} = e_1 \sigma^i \otimes I + e_2 I \otimes \sigma^j + e_3 \sigma^k \otimes \sigma^l, \tag{S66}$$

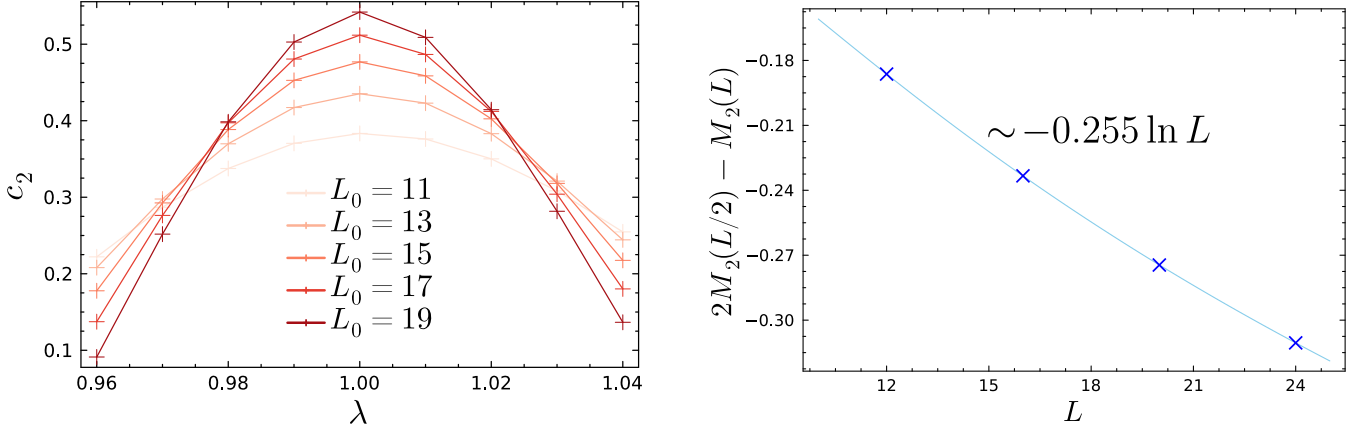


FIG. S1. (Left) Finite-size scaling of the constant term c_2 extracted from the SRE of the Ising model with the candidate defect $H_{L1} = -Z_L - X_1 - X_L Z_1$. The lack of data collapse at the critical point signals that the defect is not topological. (Right) Extraction of the logarithmic term from the difference $2M_2(L/2) - M_2(L)$. The estimated coefficient ≈ -0.255 is close to the value $-1/4$ characteristic of factorizing defects (open boundaries).

where the coefficients take values $e_1, e_2 \in \{0, \pm 1\}$ and $e_3 \in \{\pm 1\}$, and the operators are chosen from $\sigma^{i,j,k,l} \in \{X, Y, Z\}$. These constraints on the coefficients are physically motivated by the properties of the Clifford group. Since topological defects can typically be moved or fused via Clifford unitaries, and since Clifford unitaries map (Hermitian) Pauli strings to (Hermitian) Pauli strings with coefficients ± 1 , it is natural to consider the lattice realizations of such defects to be composed of terms with integer coefficients. Furthermore, to ensure the defect represents a valid interface within the chain, we impose the condition that H_{L1} does not decouple the chain or trivially block-diagonalize the Hamiltonian; for instance, a term like $X_L Z_1$ is excluded as it would isolate the operator Z_1 from the interaction.

Based on these criteria, we identify 648 distinct candidate defect configurations. To efficiently analyze these candidates, we classify them into equivalence classes based on Clifford unitaries. Specifically, we consider the local Clifford group $G = \langle S_L, S_1, CZ_{L,1} \rangle$ that preserves the form of the neighboring bulk interaction terms ($Z_{L-1} Z_L$ and $Z_1 Z_2$) by mapping the boundary Z operators to $\pm Z$. Here, S_L, S_1 are the phase gates acting on sites L and 1 , respectively, and $CZ_{L,1}$ is the controlled- Z gate between these two sites. This classification reduces the vast search space of 648 candidates to 44 distinct equivalence classes, which include the identity defect ($-X_L - X_1 - Z_L Z_1$), the η defect ($-X_L - X_1 + Z_L Z_1$), and the duality defect ($-X_L - Z_1 - X_1 Z_L$).

We then determine the topological nature of each candidate by analyzing the finite-size scaling of the SRE, $M_\alpha(L)$. The SRE serves as a sensitive probe for the properties of the defect. If the defect is topological, the SRE must exhibit a universal size-independent subleading term, c_α^A , governed by the g -factor of the boundary state Γ_1 in the \mathcal{A} defect sector. This is manifested as a clear data collapse of the constant term across different system sizes near the critical point. Conversely, if the defect corresponds to or flows to a non-topological defect, the geometry of the replicated partition function after the folding acquires sharp corners. This results in a universal logarithmic correction to the SRE.

To demonstrate this approach, we analyze a specific candidate defect given by $H_{L1} = -Z_L - X_1 - X_L Z_1$, which does not correspond to any known topological defects. We first test the hypothesis that the defect would be topological by fitting the $\alpha = 2$ SRE data to the form $M_2(L) = m_2 L - c_2 + r/L$. As shown in Fig. S1, the extracted constant c_2 shows significant finite-size dependence and fails to exhibit data collapse, indicating the defect is not topological. Subsequently, we test for the presence of a logarithmic contribution by computing the difference $2M_2(L/2) - M_2(L)$, which isolates the logarithmic term in leading order. The results in Fig. S1 reveal a logarithmic dependence with a coefficient of approximately -0.255 . This value is close to the theoretical value of $-1/4$ expected for factorizing defects. This suggests that the defect either flows to a factorizing defect in the IR limit, or is a non-topological, non-factorizing defect for which the BCCO involving Γ_1 has the same scaling dimension as that of the factorizing defects.

Once the lattice realizations of topological defects are systematically identified, their fusion rules can be determined by exploring the action of Clifford unitaries. Let $\{D^1, D^2, \dots, D^m\}$ be the set of identified topological defects. Suppose that we have the adjacent defects D_{L1}^i, D_{12}^j . To identify the fusion rule of these two defects, we exhaustively apply all possible Clifford unitaries to this defect term and calculate the resulting expression; note that the number of distinct Clifford unitaries acting on two sites is 11, 520 and on three sites is 92, 901, 120, which is always finite. We terminate this search process if either of the following results is obtained:

1. The transformed term matches one of the lattice realizations of topological defects, say D^k . This outcome confirms the fusion rule $D^i \otimes D^j = D^k$.
2. A Clifford unitary decouples a few sites, and the remaining terms match the expressions of topological defects $\{D^{k_1}, D^{k_2}, \dots, D^{k_l}\}$. This outcome confirms the fusion rule $D^i \otimes D^j = D^{k_1} \oplus D^{k_2} \oplus \dots \oplus D^{k_l}$. For instance, the fusion rule $(\mathcal{D} \otimes \mathcal{D} = \mathcal{T}^-(1 \oplus \eta))$ corresponds to a Clifford unitary decoupling a single site Z_1 with the remaining terms being the identity $(-X_L - X_2 - Z_L Z_2)$ and the η defect $(-X_L - X_2 + Z_L Z_2)$.

We emphasize that, since the number of Clifford unitaries is finite and each calculation of the transformation is computationally inexpensive (due to the Gottesman-Knill theorem), this is a practical approach to finding the fusion rules. Importantly, this method of finding the fusion rules is guaranteed to terminate. This procedure establishes a practical and rigorous method to discover the algebraic structure of generalized symmetries directly from lattice Hamiltonians.